UNITED STATES
DEPARTMENT OF THE INTERIOR
GEOLOGICAL SURVEY

CR-123596

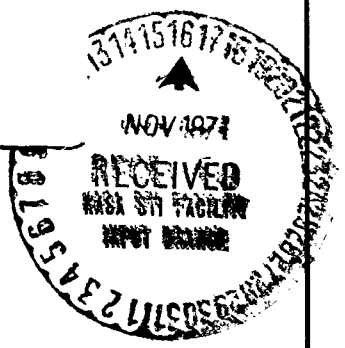

This report is preliminary and has not been edited or reviewed for conformity with U.S. Geological Survey standards and nomenclature.

Prepared by the Geological Survey for the National Aeronautics and Space Administration

14
CAT.

INTERAGENCY REPORT: 40

Evaluation of the MSFC Facsimile Camera System as a Tool for Extraterrestrial Geologic Exploration

by

E. W. Wolfe and J. D. Alderman
U.S. Geological Survey

October 1971

Prepared under NASA contract number H82013A

CONTENTS

EVALUATION OF THE MSFC FACSIMILE CAMERA SYSTEM AS A TOOL FOR EXTRATERRESTRIAL GEOLOGIC EXPLORATION

by

E. W. Wolfe and J. D. Alderman

ABSTRACT

Utility of the Marshall Space Flight Center (MSFC) facsimile camera system for extraterrestrial geologic exploration was investigated during spring 1971 near Merriam Crater in northern Arizona. Although the system with its present hard-wired recorder operates erratically, the imagery showed that the camera could be developed as a prime imaging tool for automated missions. Its utility would be enhanced by development of computer techniques that utilize digital camera output for construction of topographic maps, and it needs increased resolution for examining near field details. A supplementary imaging system may be necessary for hand specimen examination at low magnification.

INTRODUCTION

Surface imaging systems in extraterrestrial exploration will provide (1) new information in areas where orbital and telescopic photographs are unavailable, (2) new perspectives on features previously seen only from orbit or by telescope, and (3) detailed information unavailable at telescopic or orbital photographic scales. The surface imaging system will be the single most important tool for fulfilling the immediate objectives of geologic investigation of lunar and planetary surfaces. These objectives are:

1) to characterize the surface materials in terms of composition, texture, form, and distribution;
2) to classify the materials at all scales into genetically significant geologic units;
3) to determine the structural and relative chronologic relations among the units;
4) to determine the modes of origin of the units;
5) to determine the processes that have modified the geologic units.

Field testing

The utility of the Marshall Space Flight Center (MSFC) facsimile camera (Table 1) for navigation and guidance (MSFC) and for geologic reconnaissance (USGS) was tested in Spring 1971 in the San Francisco volcanic field, northern Arizona.

Panoramas, many of them stereoscopic, were made from each of 34 stations occupied in an area of young basalt flows and pyroclastic deposits near Merriam Crater (Figures 1, 2). Facsimile pictures from 9 stations (Figure 1) located along a hypothetical traverse segment were selected for evaluation of the facsimile camera and to illustrate the utility of the system for geologic reconnaissance. Hycon 307 panoramic film camera photographs made from some of the stations are included for comparison. The base map (Figure 1) is an orthophotomosaic with higher resolution than is normal in the currently available orbital imagery.

Additional facsimile images were made of test targets (Figure 12) and of the artificially cratered area at the "rockpile" at the Manned Spacecraft Center, Clear Lake City, Texas (Figure 11).

Acknowledgments

Essential support in logistics and in designing and assembling the equipment necessary for successful testing was provided by R. A. Mills, B. G. Tinnin, and I. L. Wiser, of the U. S. Geological Survey, Center of Astrogeology, Field Test Systems Shop. D. W. Houchin, representing the Photographic Support Unit of the Center of Astrogeology processed all films in the field and prepared prints.

GEOLOGIC EVALUATION

In order to fulfill its role in automated geoscience exploration, an imaging system must provide the following:

1) location and guidance data;
2) discrimination of geologic units and geomorphic features;

PHILCO Ford
Philco-Ford Corporation
Aeronutronic Division
Newport Beach, California

MINIFAX CAMERA SYSTEM

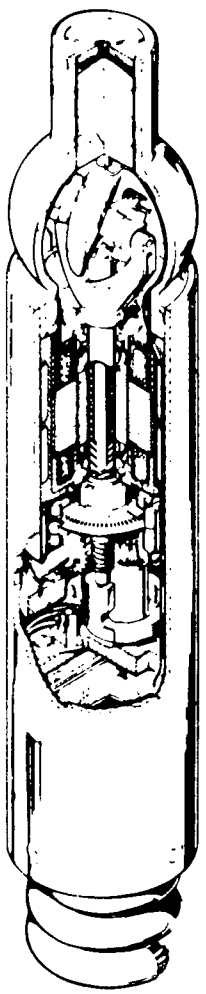

Apparent Size

MINIFAX CAMERA	
Image Field of View	+60, -30 x 360 Degrees
Scan Format	900 Horizontal Lines
Image Point Spacing	0.1 Degree
Scan Rate	30 Lines Per Sec
Data Rate	108,000 Image Points Per Sec
Frame Time	30 Seconds
Spectral Response	Silicon, 0.4 - 1.0 Micron
Noise Equiv. Brightness	25 Ft - Lamberts at 54 kHz
Dynamic Range	25 - 10,000 Ft - Lamberts
Data Synchronization	Line and Frame Sync
Scan Sync Reference	6 kHz
Operating Power	1.5 Watts @ 14 Vdc
Video Output	0 - 10 Volts
Size	1.0 In. Dia x 6.0 In. Long
Weight	0.6 Pound
Environment	1000 g Delivery Shock -10°F to +150°F Terrestrial Exposure, 1 Year

MINIFAX RECORDER	
Image Size	4.5 x 18 Inches
Record Medium	Photographic Film
Line Spacing	0.005 Inch
Line-to-Line Correlation	0.001 Inch (0.02 Degree)
Recording Dynamic Range	200/1
Operating Power	150 Watts @ 110 V, 60 Hz
Size	9 x 14 x 14 Inches
Weight	50 Pounds
Operating Features	Gain and Bias Controls Daylight Loading Real Time Recording Portable

TABLE 1

3) characterization including structural and textural detail of rock and regolith units;

4) information on spatial distribution of geologic units.

Location and guidance

Determination of vehicle location and accurate guidance of the vehicle to specific sites selected for scientific observation or instrumentation are necessary operations in automated geoscience exploration. The 360° format and high degree of angular precision permit reliable triangulation that renders the facsimile camera system excellent for navigation and guidance. This capability is documented in the concurrent MSFC Landmark Navigation Evaluation of the system.

Discrimination of geologic units and geomorphic features

Recognition of the occurrence of geologically or geomorphically distinct units provides the initial basis for geologic interpretation and for direction of sampling. In most planetary exploration we can expect discrimination of units to begin on orbital photographs. In the Merriam test area the major geologic units (e.g. lava flows, cinder cones, tuff ring, smooth cinder-covered areas) are so distinct and the quality of the aerial photography (Figure 1a) is so good that most of the geologically significant units can be discriminated on the aerial photograph. Orbital photographs of extraterrestrial surfaces will normally permit less acute discrimination of geologic features; hence the surface imaging system will play a proportionately more significant role in distinguishing geologic features and in guiding efforts to characterize and sample them.

Every panorama in the Merriam Crater area (Figures 2-10) and at the "rockpile" (Figure 11) shows that the system is capable of discriminating geologic units and geomorphic features in the middle and far fields. The system does not permit some of the distinctions that the eye can make on the basis of color nor does it permit the near field (less than 5 m) distinctions that the eye can resolve on the basis of subtle variations in color,

texture, or mineralogy.

Specific examples of the ability of the facsimile system to provide discrimination follow:

1) Figures 2a and 2b illustrate the system's utility for far field discrimination of large units. Station 4 is located on an extensive smooth dark surface that forms one of several distinctive geologic features worthy of investigation. A steep low scarp to the southeast bounds a second morphologic unit that can be interpreted in the aerial photograph (Figure 1a) as a lava flow. To the north a smooth light-colored slope forms a third unit that coincides with the south flank of the tuff ring. A black linear patch (wind-blown ash) at the base of that slope represents a fourth distinguishable unit, and a cinder cone (crater 176) behind and standing above the level of the tuff ring forms a fifth distinctive unit. Merriam Crater, to the southeast, is recognizable as a cinder cone with a fan-like constructional feature extending from its north flank. To the south, the spatter cone represents a distinctly different kind of volcanic construct, and low rounded hills on the horizon from southwest to northwest (cinder cones) may represent still additional geologic features that should be investigated.
2) Figures 5a, b, and c illustrate the type of near field discrimination of units or materials that can be achieved with the facsimile camera. Two major units--the tuff outcrop itself and the smooth fragmental material below the outcrop base (central and left part of format in Figures 5a and b)--can be distinguished. An additional unit consisting of a regolith of loose fragments on the subhorizontal part of the outcrop surface is recognized. Within the tuff (Figure 5c) it is possible to discriminate at least three kinds of material

that should be investigated--light-colored clasts, dark clasts, and the fine matrix.

3) Figures 11a and b provide an example of the local discrimination possible on the simulated lunar surface at the "rockpile". Initially the area can be divided into cratered areas and intercrater areas. The craters are divisible into smooth and blocky types, and the smooth craters can be categorized for investigation on the basis of size as determined in the stereo model by trigonometric methods. Both blocks and fine smooth regolith can be distinguished and sampled in the intercrater areas, and a variety of block types, distinguished primarily by albedo, can be discriminated and, hence, investigated and sampled in the large blocky crater.

Some geologically significant discriminations are easily made visually but are difficult or impossible to make in the facsimile records. For example important distinctions in the particulate mantle at stations 5 and 6 are uninterpretable. At station 6 (Figure 7), the large rock is surrounded by an apron of fine, black, wind-blown ash mixed with a few basalt fragments. In contrast the mantling material at station 5 (Figure 6) consists of coarser (generally 1-2 cm) weathered brown cinders of air fall origin and some basalt fragments from the lava flow top.

Characterization of rock and soil units

A major effort in terrestrial geologic field investigation is devoted to defining the character of each geologic unit at eyeball resolution in the near field, at hand lens (10x) resolution in hand specimen, and in proportionately coarser detail with increasing distance from the observer. In order to provide comparable acuity, the surface imaging system must be capable of resolving features of 0.5 mm or finer size in the near field and of 0.05 mm or finer size in selected closeup views. The

panoramas recorded in the Merriam Crater area show that the facsimile camera provides good reconnaissance detail but does not provide the level of near field or hand specimen detail that effective automated geologic exploration would require.

At the coarser levels of detail, the facsimile camera does an admirable job of providing data for characterization of rock and soil units. For example, the lava flow tops at stations 5 and 6 (Figures 6, 7) are readily interpreted as consisting of irregularly shaped angular blocks of dark rock projecting through a mantle of relatively fine particulate material. It is impossible to recognize that the blocks consist of basalt, but the interpretation that they represent the top of a basaltic aa flow is reasonable when the geologic setting as seen in the aerial photograph (Figure 1a) and in the group of panoramas is considered.

The series of panoramas from stations 1, 2, and 3 (Figures 3, 4, and 5a-c) provides good examples of the utility of the facsimile camera for permitting characterization of the unconsolidated fragmental regolith within the tuff ring and also of the lithology and structure of the tuff outcrop in successively closer views. Stereoscopic viewing of Figures 5a and b greatly enhances the structural and textural detail that can be interpreted. The facsimile images show that the unit is a fragmental rock with angular clasts of more than one rock type in a relatively fine matrix. It is gently dipping and is characterized generally by well developed planar bedding, but local low-angle cross bedding occurs. It is clearly unique among the units observed elsewhere in the area. The above characterization in combination with both the outcrop pattern determined from the aerial photograph (Figure 1a) and the volcanic setting that can be interpreted from the aerial photograph and the suite of facsimile panoramas provides the basis for recognizing the outcrop as part of a ring of tuff that may represent the beds deposited on the rim of a volcanic maar. Such interpretation is

highly significant because maar rim deposits include abundant debris derived from depth in the underlying bedrock and thus provide a means of sampling subsurface materials.

Figures 5a and b and Figure 5c yield a measure of the near field resolution of the facsimile camera system. The smallest identifiable clasts in Figures 5a and b, in which the nearest part of the outcrop is about 4.5 m distant, are about 1 cm in diameter. In Figure 5c, in which the nearest part of the outcrop is about 1 m away, the smallest identifiable clasts are approximately .25 cm in diameter. These minimum clast sizes correspond to an angular resolution of approximately .14°. Much of the rock consists of glassy basaltic clasts that are unresolvable in the facsimile images. They are similar in size to the white clasts, but they contrast poorly with the matrix, which is similar in color.

Although the facsimile camera permits a high degree of lithologic characterization of the tuff in the near field, it does not approximate the detail that is apparent to the eye or to a relatively high resolution film camera. Better approximations of the outcrop character are recorded in Figure 5d, a partial panorama made with a hand-held Hasselblad film camera, with the nearest part of the outcrop about 4 to 5 m from the camera, and Figure 5e, in a Hasselblad view from 1.5 m. Figure 5f is an actual-size stereoscopic view of the tuff made with the Apollo lunar surface closeup stereo camera. The closeup stereo camera view extends perception into the relatively high resolution range that would be required for automated geologic exploration. It is worth noting that stereoscopic viewing greatly facilitates geologic interpretation at the high resolutions of sample inspection as well as at the lesser resolutions appropriate for geologic reconnaissance.

Spatial distribution of geologic units

Geologic chronology, vital to our understanding the evolution of any planetary surface, is interpreted in large part from

the spatial relations of geologic units. Defining these relations in the field and portraying them on geologic maps and cross sections make up a major portion of the effort in terrestrial geologic investigations.

In automated exploration, the imaging system complemented by the information that can be gleaned from orbital photographs is the geologic mapping tool. High quality stereoscopic orbital coverage would greatly simplify the mapping process and increase the overall effectiveness of the automated exploration project, but high quality stereoscopic orbital photographs are likely to be unavailable for some areas. Hence the imaging system may bear the brunt of providing data on spatial distribution of geologic features.

The facsimile panoramas produced in the Merriam Crater area are not adaptable to standard photogrammetric mapping techniques. However, they are excellent for triangulation and for trigonometric determination of the geometry, size and spatial relations of geologic features. Even without the airphoto base (Figure 1a) it would be possible, utilizing overlapping panoramic views from a variety of perspectives, to construct a good--albeit incomplete--map showing the distribution of geologic and topographic features in the traverse area.

In addition to fulfilling the more-or-less mechanical mapping requirements, the facsimile system provides sufficient geometric data, particularly in stereoscopic views, for geologic interpretation at all but the highest resolutions.

Figure 8, a far field stereo pair constructed from panoramas at successive stations 140 m apart, shows the shapes and spatial relations of Merriam Crater and the fan-like construct to its north insofar as they can be seen from the perspectives of stations 6 and 7. It is possible from this stereo pair to prepare a map that shows the shape, size, and distribution of the features visible on the stereo model. (Heights determined trigonometrically from the facsimile imagery for Merriam Crater

and for the scarp that bounds the fan-like construct on its west side are well within 10 percent of their actual values). The stereo pair also provides for geologic interpretation vital in directing sampling and in evaluating analytical results in terms of the geologic evaluation of the area. Merriam Crater is clearly recognizable as a cinder cone. Interpretation from the model correctly suggests that the "fan" is a lava flow that issued from a vent on the north side of the cinder cone after the cone had essentially attained its present size and shape. In fact the flow is largely mantled by cinders sprayed onto its surface during its extrusion from the vent--a fact that would have been discovered by close automated inspection.

Figures 5a and b comprise a near field stereo pair constructed from successive panoramas with a vertical perspective difference of 83 cm. Trigonometric techniques are capable of producing from the pair a precise topographic and geologic map of a portion of the outcrop showing the size, shape, and distribution of its clasts and structures. Geologic interpretations from the stereo model provides a context--including age relations--for sampling. The outcrop consists of consolidated, well bedded, gently dipping, partially cross bedded, poorly sorted, fragmental material with several clast types. At its base the outcrop is clearly overlain by unconsolidated fragmental material that occurs in the uppermost part of whatever fills the topographically low area in the left half of the format. A thin layer of unconsolidated material that is presumably a lag of debris weathered from the outcrop rests on a subhorizontal surface low in the outcrop.

TECHNICAL EVALUATION AND RECOMMENDATIONS

System performance

Based on our field experience with the MSFC facsimile camera system, we feel that the camera is an acceptable bread-board model, but that the recording system is deficient. In the one instance where the camera was subjected to extended solar heating, the rate of mirror rotation decreased perceptibly. Otherwise, no problems specifically attributable to camera function were identified.

The recording system is apparently extremely sensitive to its environment. Changes in temperature, atmospheric pressure, and humidity seem to spell the difference between an acceptable image or varying degrees of failure due largely to loss of camera-recorder synchronization. The success rate near sea level in the warm humid climate at the Houston "rockpile" was approximately three times that at a mile above sea level in the very dry climate of the Merriam Crater area.

The inadequacies of the tested recording system emphasize the need for development of a superior recording system for use in advanced research and development. A permanent magnetic tape recording of the camera output and display equipment would permit reproduction of data to which currently undeveloped techniques for image enhancement and format correction could be applied.

Camera and format characteristics

Format characteristics were determined utilizing the Viking test ranges (Figure 12). The test range dimensions are 4 x 8 feet. The ranges can be rotated from vertical to horizontal.

Test Range B has a precision grid with 200 intersections on 127.04 mm centers. The intersections are marked by high contrast decals that are either white on black or black on white on the neutral background of the range. The decals have 1, 2, 4, and 8 mm diameter spots.

Test Range A consists of:

1) Air Force resolution bar chart
2) Two NBS calibration targets
3) A scribe coat (orange) grid with 90 cm centers marked by high contrast black on white and white on black decals with 1, 2, and 3 mm spot sizes.
4) Seven Munsell color chips (bottom set on test range: 7.5P5/10, 7.5B5/6, 5G5/8, 5GY7/10, 5Y8/12, 5R5/12, 5YR6/12).
5) Various 3-dimensional geometric figures on a non-reflecting black background.
6) Munsell chips representing 16 gray levels (top set on test range: N2/, N3/, N4/, N5/, N6/,N7/, N8/, N9/), (middle set on test range: N2.5/, N3.5/, N4.5/, N6.5/, N7.5/, N8.5/, N9.5/).

The camera was set up to have the test range fill as much of the format in vertical dimension as possible, but this was limited by camera depth of field. In recording the scene used for measurements (Figure 12), the leveled camera was located 1511 mm from test range B along a normal to the center of the test range. Camera height of 1127 mm coincided with the test range center. Distance to the center of the grid on test range A was 1582 mm. Reductions of Mann comparator measurements gave the following results:

Usable focal length - 73.777 mm

Usable format dimensions - 457 x 115.6 mm

Horizon is 39.75 mm from bottom edge of format

Equivalent horizontal focal length - 73.810 mm

Equivalent vertical focal length - 73.430 mm

(Differences in horizontal and vertical focal lengths probably result from film distortion)

Scan width (center to center) - 0.1265 mm

Figure 13 is an isodensity tracing of the upper gray scale. Values are related to variable factors such as film sensitivity and film processing as well as to facsimile camera characteristics.

However, the data show that in spite of its operating deficiencies, the system discriminates all 8 gray scale chips.

The tested camera scans from 30° below horizontal to 60° above horizontal. A greater downward view, perhaps as much as 60° below horizontal, would be preferable, and upward view could be reduced. In a two-camera, vertical base stereo system, it would be desirable to adjust the field of view so that the bottom edges of the simultaneous formats coincide.

Theoretical angular resolution of the MSFC facsimile camera system is 0.1°. Some high contrast objects with angular widths of about 0.14° were recognized on images made in the field (Figures 5a, b, and c). Maximum practical resolution would be desirable. An increase in angular resolution to .05° would significantly enrich the near field data content. Previous studies of electro-mechanical scanning devices (J. D. Alderman, unpublished data) indicate that an angular resolution of .05° is a reasonable goal.

Trigonometric measurements

Computations of heights of features or their distance from the facsimile camera are based upon measured format characteristics and simple trigonometric relationships. The bottom edge of the format, 39.75 mm or 31.6° below the horizon when the camera is vertical, provides a reference for measuring vertical angles. One degree is approximately equivalent to 1.265 mm in the format.

A bullseye bubble was used to orient the camera in the field. With the camera properly plumbed, computed values for range or height were within 10 percent of actual values. In a camera system with 0.1° angular resolution, errors in camera orientation should not exceed 0.1°.

With vertical stereo base, range to a point and the height of the point relative to the camera can be computed. Ideally the ratio of range to base should be less than 40. The two camera positions and the point in the format are the apices of a tri-

angle in which all angles can be calculated from the vertical angles determined by measurement of the angular distance in the format from the horizon to the point. The known camera separation provides the length of one side of the triangle. The other sides can be determined by application of the sine law and, hence, the spatial relations between the point and the camera are calculable.

Single photo measurements of the height of a point relative to the camera are possible utilizing the vertical angle determined in the format and the range measured from a base map such as an orbital photograph. In the absence of a base map of suitable quality, range to a point can be determined from successive panoramas if distances between camera stations are known.

Stereoscopy

Stereoscopic models utilizing conventional photographs are widely used for visual scientific interpretation and with optical plotters for efficient measurement and mapping. The MSFC facsimile camera system provides imagery suitable for qualitative interpretation, but further development of effective mapping techniques is needed.

Measurement and map construction.--For several reasons, measurements and map constructions utilizing standard photogrammetric techniques are impractical with the MSFC facsimile camera system data. The major problems are:

1) A facsimile picture is considered to be a simple cylindrical projection. Most photogrammetric plotting instruments are designed for use with conventional photographs, which are plane-perspective projections. The effect is that the parallax-free stereoscopic model required for optical data reduction cannot be established with facsimile images.
2) The difficulty in establishing a parallax-free model is compounded by the changing perspective center from one

scan line to the next. The perspective center is the basic photogrammetric reference point, and normal fixed-frame photographs have a single perspective center.

3) Under the magnification of optical photogrammetric instruments, the discontinuities between adjacent scan lines dominate the field of view creating a screening effect that makes image-matching difficult.

4) Small scale distortions such as inaccuracies in relative horizontal positioning of successive scan lines (which would result in slight offset at scan boundaries in the display of a vertical line) are introduced by both imaging and playback systems. These are quite unlike the radial optical distortions present in conventional photographs and would cause additional difficulty in establishing a parallax-free model. Degraded photogrammetric measurement would result even if the other problems (1, 2, 3) could be eliminated.

The results of this experiment suggest that it is impractical to attempt to adapt optical photogrammetry to reduction of data from this type of imagery. Detailed reduction of massive data would best be accomplished by digital computation employing an object space coordinate system for individual sets of conjugate points. Precise control of format accuracy and repeatability, an internal reference system (analogous to the fiducial marks of an aerial film camera), careful calibration of major system components, and precise camera orientation, particularly relative to vertical (probably determined celestially), are vital factors in optimizing data value. In addition, image reconstruction in the best form possible is mandatory for visual scientific interpretation.

Vertical stereo.--Vertical base stereoscopic models offer some significant advantages with this type of unrolled cylindrical format. Computational accuracy is acceptable as long as the ratio of range to base is less than 40. Format rearrangement for full 360° stereoscopic viewing is minor for vertical base models (e.g. Figures 5a and b) in comparison with horizontal base models, which are cumbersome to handle with a normal stereoscope and in which large scale changes, especially in the near field, impede image correlation. In addition, there is no loss of stereo in vertical base models due to common viewing axis.

The 90° rotation from normal that a vertical base requires for stereo viewing is a minor invonvenience to which the photointerpreter can adapt.

Good photogrammetric control in automated missions could be achieved by using small vertical base stereo models at single stations to help control large horizontal base stereo models constructed from panoramas at successive stations. For optimum photogrammetry we recommend that a two camera system with fixed vertical base be employed.

CONCLUSIONS

The major results of evaluation of the geologic utility of the MSFC facsimile camera system for automated planetary exploration can be summarized as follows:

1) Because of its 360° format and degree of angular precision, the MSFC facsimile camera system provides reliable triangulation; hence it functions well as a tool for navigation and guidance.
2) Resolution, format geometry, and gray scale response permit discrimination of most geologic units significant at reconnaissance scales in the test area.
3) Panoramas recorded in the Merriam Crater area contain

sufficient information to permit adequate characterization of geologic units at all ranges except at the level of near field (less than 5 m) and hand specimen detail. Detail at all scales is enhanced by stereoscopic viewing. Near field detail would be more nearly sufficient if angular resolution of the system were doubled (i.e., if the angular resolution were .05°).

4) In its current configuration with the camera hard-wired to an analog film recorder, the system operates erratically, and the data it produces are commonly substandard. Presumably this problem would not exist in planetary exploration, where correct camera output could be transmitted to earth in digital form.

5) The geometry of the system precludes application of standard photogrammetric procedures for measuring and mapping. However, measurements and production of maps are currently feasible utilizing triangulation and trigonometric calculations. Spatial relations of geologic features are qualitatively interpretable in stereoscopic views. Hence the system is capable of providing base maps on which geologic relations can be portrayed.

6) Mapping capability could be significantly enhanced by application of computer techniques to digital data derived directly from the camera. Providing format accuracy is precisely controlled, an internal reference is built into each camera, major system components are carefully calibrated, and camera orientation is precisely known, digital data adequate for production of well controlled maps could be generated by a two camera system in which the cameras were rigidly fixed relative to each other.

REFERENCE

Colton, H. S., 1967, The basaltic cinder cones and lava flows of the San Francisco Mountain Volcanic Field: Museum of Northern Arizona, Flagstaff, Arizona, 58 p.

CAPTIONS FOR ILLUSTRATIONS

Figure 1A. Index map. Orthophotomosaic identifying the major topographic features of the Merriam Crater area. Numbers identify camera stations to which this report refers. Surface features are predominantly young (Pleistocene of Recent) volcanic cones and lava flows locally mantled by deposits of cinders and ash. As per common local usage, the term crater is applied to all cinder cones whether or not a depression occurs at the crest. Crater numbering system after Colton (1967).

Figure 1B. Index map. Topographic map of the Merriam Crater area.

Figure 2 (a,b). Stereoscopic facsimile panorama from station 4 showing the major topographic features identified in Figure 1. Horizontal base separation = 1.5 m along bar shown near bottom center of Figure 2b. Effective base separation approaches zero along the azimuth from the center of the spatter cone through station 4 to the vans parked on the south rim of the tuff ring (i.e. parallel to the bar in Figure 2b). Use Figure 2b as the left member of the stereo pair for areas to the left of the vans and as the right member of the stereo pair for areas between the vans and the center of the spatter cone near the right hand edge of the pair of images. Foreground surface consists of loose cinders that are not resolved in this pair of images. Stereoscopic view to the southeast toward station 5 (using Figure 2b as right hand member of stereo pair) shows a small gully (occupied by road) between the facsimile camera and the lava flow front, and it shows the sharp relief on the flow front at a distance of about 255 m. Trigonometric determination of the flow front height--about 3 m--in Figure 2a is in good agreement with the height observed in the field. Linear diagonal pattern is an artifact produced in halftone reproduction.

Figure 2C. Photographic panorama made with Hycon 307 aerial panoramic camera at station 4.

Figure 3. Facsimile panorama from station 1. The low ridge on the horizon in the central part of the format is the northeast rim of the tuff ring, which, at its nearest point, is about 100 m from the facsimile camera. The low topographic profile and layering expressed by cavernous weathering of the tuff are evident. At the far left (north to northwest) are outcrops of the Crater 176 lava flow, that overrides the tuff. The distance to the base of Crater 176 is approximately half a kilometer. The base of Merriam Crater at the right (southeast) is approximately 2 km distant. Linear diagonal pattern is an artifact produced in halftone reproduction.

Figure 4. Facsimile panorama from station 2. Merriam Crater is in the distance at the center. A segment of the northeast rim of the tuff ring forms a local horizon in the left central part of the format. Layering of the tuff is distinctly visible. The fragmental texture of the surface material in the foreground is also evident. Boulder identified in figure 5 is discernible but difficult to identify. Linear diagonal pattern is an artifact produced in halftone reproduction.

Figure 5. (5a-bottom; 5b-top). Stereoscopic facsimile panorama from station 3. Vertical base separation = 83 cm. View of a segment (see Figure 4) of the northeast rim of the tuff ring in right half of format. Facsimile camera is approximately 4.5 m from nearest part of tuff ring. Details of general outcrop morphology and fabric, including layering, cavernous weathering, occurrence of white and dark clasts in a finer irresolvable matrix, and development of a regolith of coarse dark and white fragments on the sub-horizontal outcrop surface in the right foreground, are excellent. The large rounded boulder included in the tuff near the left end of the outcrop (see also Figure 4) is seen in the field to

Figure 5 (continued)-- be a red sandstone boulder 74 x 60 cm in cross section. It is 12 m from the camera. Visual observations show that the dark clasts are predominantly basalt fragments and the white clasts are inclusions of older limestone. Minimum resolvable size of white limestone clasts is about 1 cm. Linear diagonal pattern is an artifact produced in halftone reproduction.

Figure 5c. Closeup facsimile panorama showing tuff ring near station 3. Facsimile camera approximately 1 m from nearest part of tuff outcrop. Although this part of the outcrop is slightly out of focus, comparison with Figures 5a, b shows that details of the occurrence of clasts and their relation to the matrix are significantly enhanced. Minimum resolvable size for white limestone clasts is approximately .25 cm. Linear diagonal pattern is an artifact produced in halftone reproduction.

Figure 5d. Partial Hasselblad (60 mm focal length) photographic panorama of a portion of the tuff ring near the area of Figures 5a-c. Nearest part of outcrop approximately the same distance (4-5m) from the camera as the nearest part of the outcrop in Figures 5a and b.

Figure 5e. Hasselblad (60 mm focal length) photograph of a portion of the tuff ring outcrop. Camera approximately 1.5 m from the outcrop.

Figure 5f. Stereoscopic pair made with the Apollo lunar surface closeup stereo camera. Shows detail of tuff at approximately actual size. Light-colored clasts are limestone; dark clasts are largely vesicular porphyritic red basaltic cinders. Clasts as small as 0.1 mm are recognizable. The matrix consists of sand and silt from shattered bedrock mixed with finely comminuted glassy basalt debris.

Figure 6 (a,b). Stereoscopic facsimile panorama from station 5. Horizontal base separation = 1.5 m along bar shown at bottom center of Figure 6b. Effective base separation approaches zero along azimuth from station 5 to center of Merriam Crater and at edges of format (i.e. parallel to the bar in Figure 6b). Use Figure 6b for left member of stereo model for areas to left of Merriam Crater and for right member of stereo model for areas to right of Merriam Crater.

Station 5 is located about 1.3 km from the base of Merriam Crater on the surface of a lava flow. The stereo model shows good detail of the irregular flow top characterized by angular protuberances of aa-type lava projecting through relatively smooth but clearly fragmental mantling material known from visual field observation to consist of basaltic cinders. Arrow points to the large rock at station 6 (Figure 7). Linear diagonal pattern is an artifact produced in halftone reproduction.

Figure 6c. Photographic panorama made with Hycon 307 aerial panoramic camera at station 5.

Figure 7 (a,b,c). Partial facsimile panoramas (approximately 200° wide) including the large rock at station 6. Figures 7a and 7b from same camera position. Figure 7a with facsimile camera vertical, 7b with camera tilted 10-15° from vertical. Figure 7c is the upper member of a vertical stereo pair using either 7a or 7b as the lower member. Vertical base separation = 184 cm. Station 6 is located on the surface of a lava flow similar to that at station 5 but characterized here by larger blocks. The rubbly aa texture of the congealed lava blocks, crude layering in the large central block, and loose fragmental character of the mantling cinders and ash are evident. Note the detailed tread pattern in the vehicle tracks in the left hand portion of the format. Distance to prominent nearby features is labelled in Figure 7a.

Figure 7 (a,b,c). (continued)

Tilting of the camera 10-15° results in a weak stereo model. When the correct viewing position (correct base alignment) is used, the stereoscopic view enhances interpretation, particularly in the near field. The very small base separation achieved by tilting results in a stereoscopic model that is useful for qualitative interpretation but not for measurement.

Figure 7d. Partial photographic panorama of large rock at station 6. Picture reproduced from a single 40° x 130° frame taken with Hycon 307 aerial panoramic camera.

Figure 8. Facsimile stereoscopic view of Merriam Crater. Left hand member of pair from a panorama at station 6; right hand member from a panorama at station 7. Base separation is approximately 140 m. Distance to base of Merriam Crater is approximately 1.5 km. Numbers show height in meters of scarp at edge of fan-like volcanic construct north of Merriam Crater.

Figure 9a. Facsimile panorama from station 8. Image shows the rubbly character of the surface between the station and the near base of the spatter cone approximately 115 m away. It shows the profile of the spatter cone normal to its long axis--information not available from the photo base (Figure 1) itself, and it also provides a good perspective of the blocky lava flow surfaces to the northeast. Arrow points to the large rock at station 6 approximately 400 m distant. Linear diagonal pattern is an artifact produced in halftone reproduction process.

Figure 9b. Photographic panorama at station 8. Panorama compiled from pictures made with Hycon 307 aerial panoramic camera.

Figure 10 (a,b). Stereoscopic facsimile panorama from station 9. Vertical stereo: base separation approximately 100 cm. Figure 10a is the lower member of the stereo pair, Figure 10b the upper member. Station 9 is located in a low saddle in the northeast wall of the spatter cone. Most of the stereo panorama shows the wall adjacent to the saddle and the interior of the spatter cone. Blocky lava that flowed northeast from the breach at station 9 can be seen near the left end of the image pair. The near wall (near image center) is shown to consist of cobble-sized rubble that is probably loose. This rubble is part of a smooth surface that mantles the crater floor, the floor of the saddle, and the wall northeast (far right part of image pair) of the saddle. Outcrops of dark rock project through this mantle in places along the interior walls; this material would probably be accessible to an automated vehicle in the wall northwest of the saddle and in the near wall where blocks may have rolled or slid downslope (image center). Smooth dark material mantles the southwest interior wall and can be determined in the stereo model to be accessible to an automated vehicle.

Visual observations show that the spatter cone consists of consolidated layered basaltic spatter partly mantled by cinders and loose spatter material. The floor is mantled by basaltic cinders, and the dark material along the far wall is a deposit of fine black wind-blown volcanic ash.

Trigonometric determinations based on Figure 10a and on the map distance from station 9 to the southwest wall of the spatter cone, approximately 360 m distant at its crest, indicate that the southwest wall is approximately 270 feet high. Approximate height interpreted from the topographic map is 250 feet. Linear diagonal pattern is an artifact produced in halftone reproduction.

Figure 10c. Photographic panorama at station 9. Panorama compiled from pictures made with Hycon 307 aerial panoramic camera.

Figure 11 (a,b). Stereoscopic facsimile panorama at "the rock-pile", Manned Spacecraft Center, Clear Lake City, Texas. Vertical stereo: base separation = 42.5 cm. Figure 11a is lower member of stereo pair (camera height 114.3 cm); Figure 11b is upper member (camera height 156.8 cm). Morphology of craters and blocks simulating a lunar or planetary surface is easily interpreted in the stereo model. Trigonometric calculations utilizing the stereo base indicate a depth of 4 m and diameter of 13 m for the large blocky crater in the foreground. Linear diagonal pattern is an artifact produced in halftone reproduction.

Figure 12. Viking test ranges.

Figure 13. Isodensity tracing from right to left on upper gray scale (top row of chips) shown on test range A in Figure 12. Numbers identify density records of chips (white = 1; black = 8).


Figure 1a
CRATER 176
N
1
2
3
CRATER 236
TUFF RING
4
FLOW FRONT
5
6
7
8
MERRIAM CRATER
SPATTER
9
CONE
CRATER 234
CRATER 177
0
1000 METERS

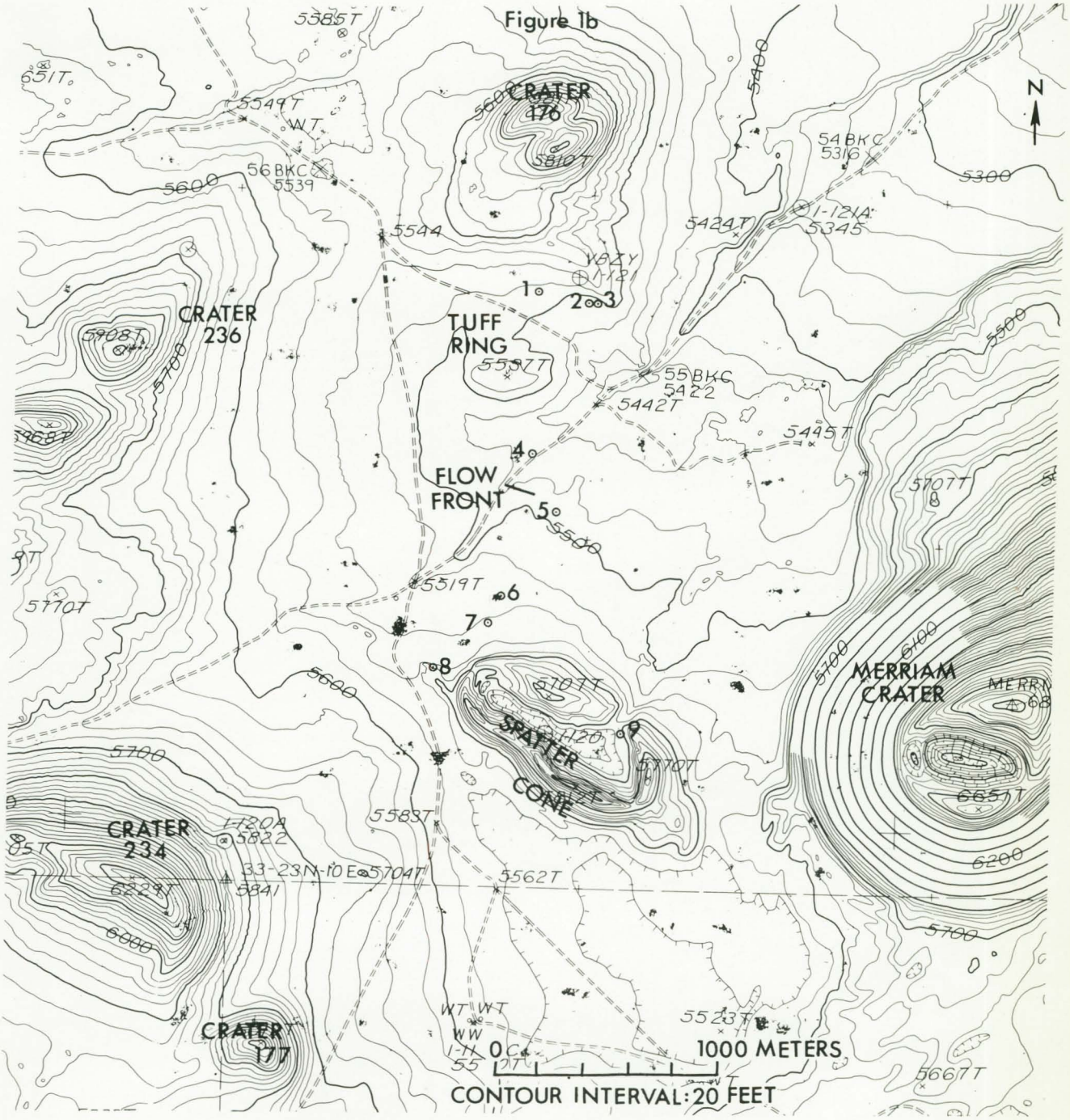
Figure 1b
CRATER 176
CRATER 236
TUFF RING
FLOW FRONT
SPATTER CONE
CRATER 234
CRATER 177
MERRIAM CRATER
N
1000 METERS
CONTOUR INTERVAL: 20 FEET

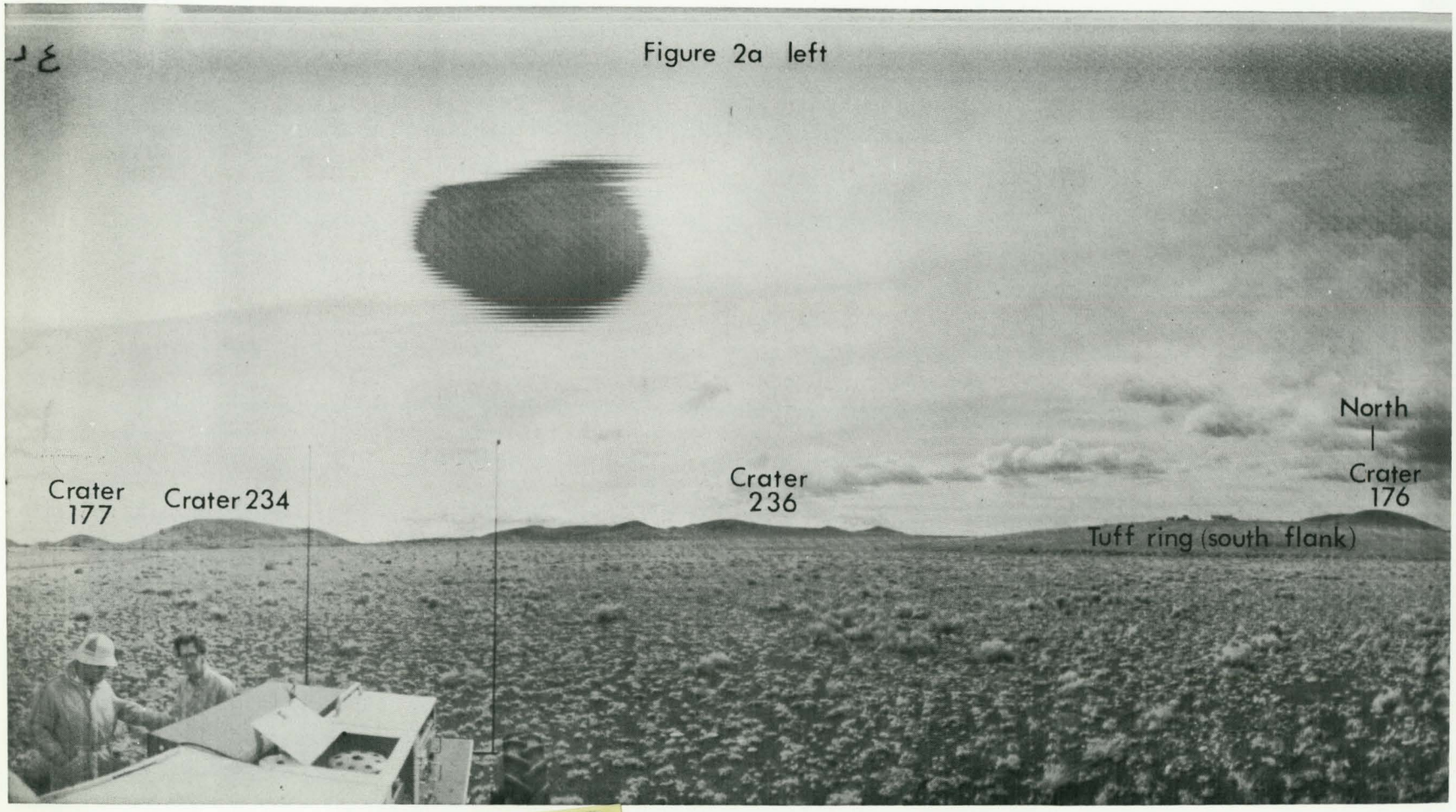

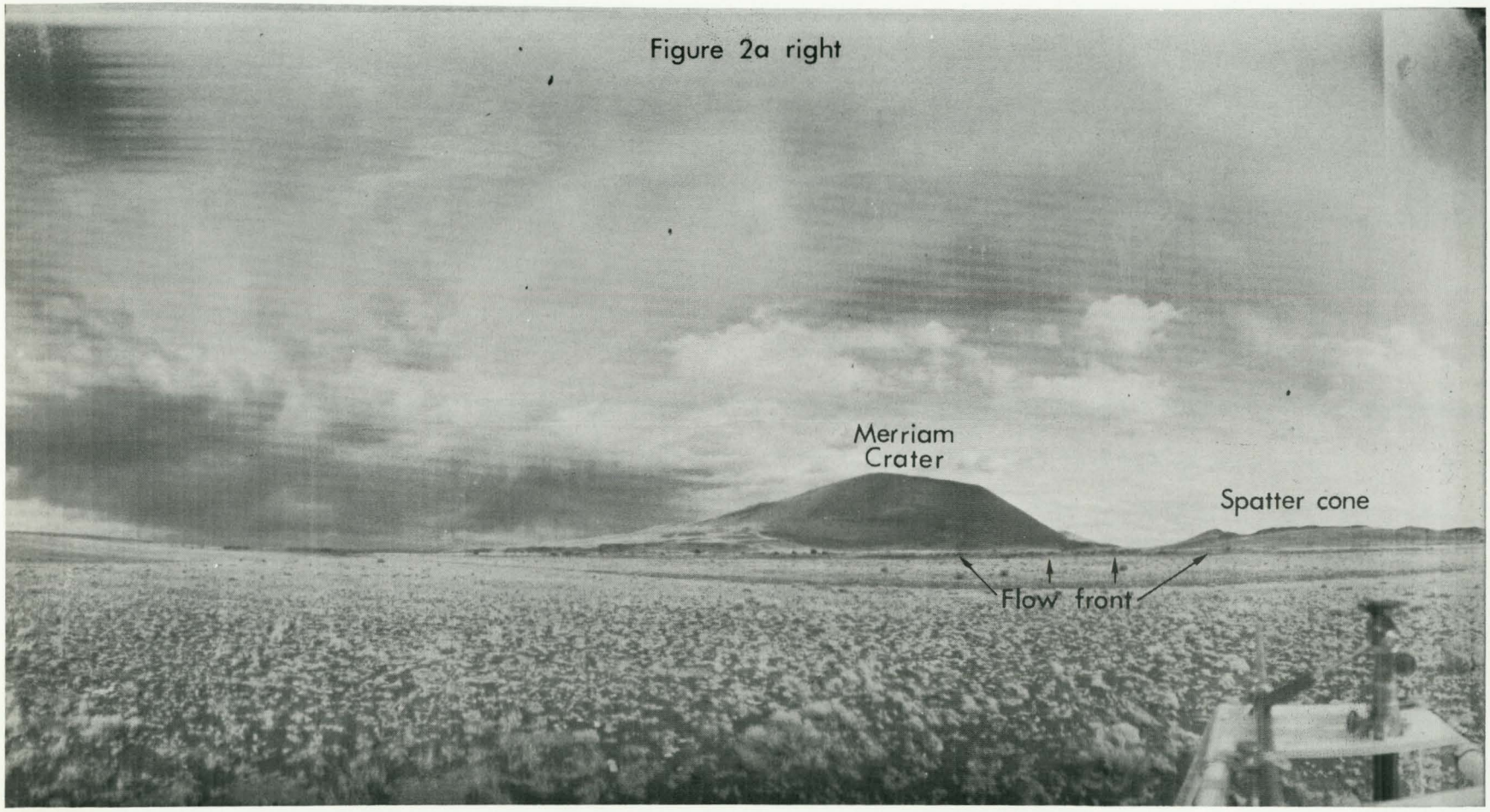
Figure 2a right
Merriam
Crater
Spatter cone
Flow front

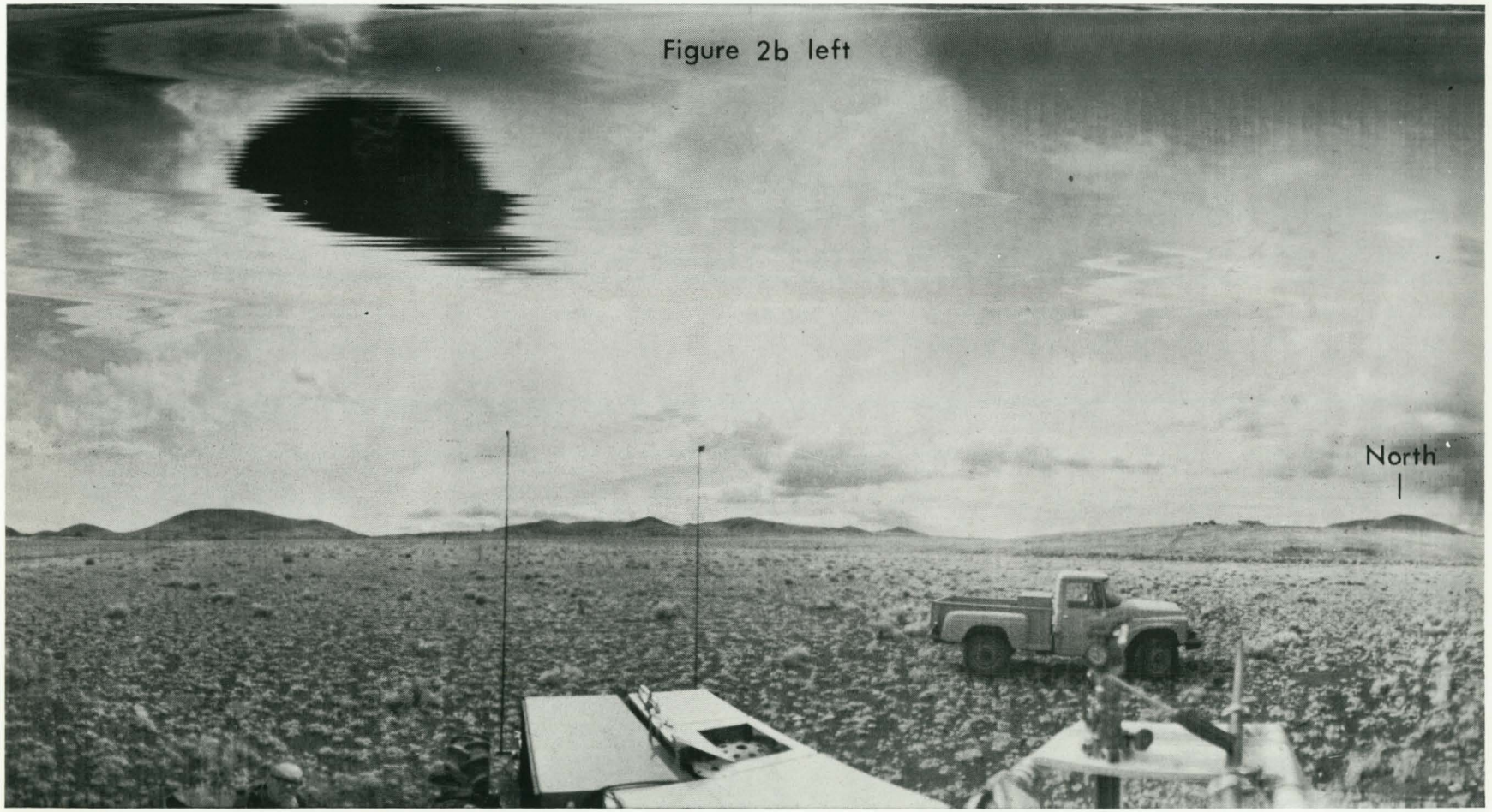


Figure 2b right

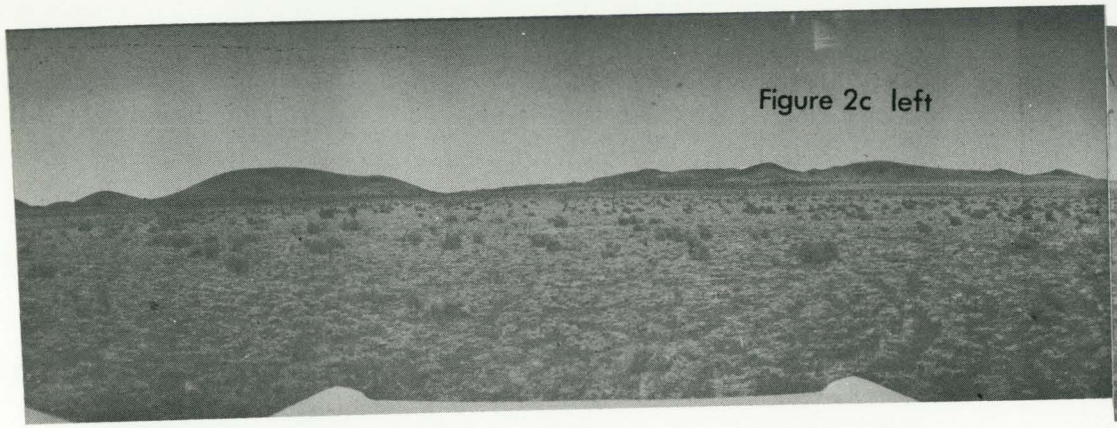

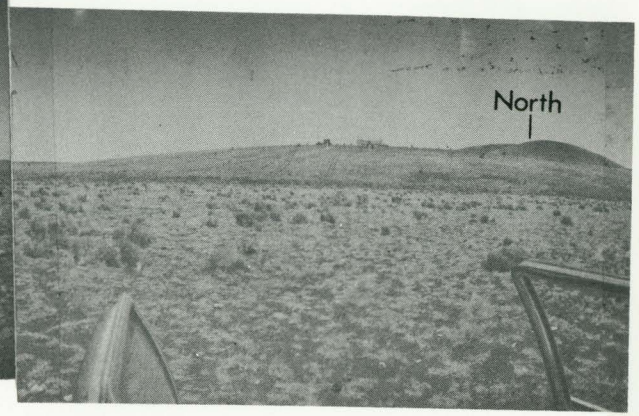

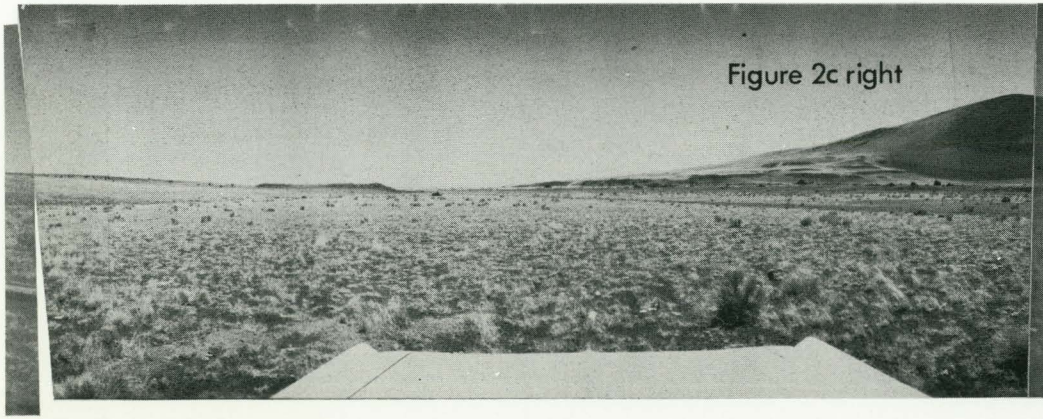

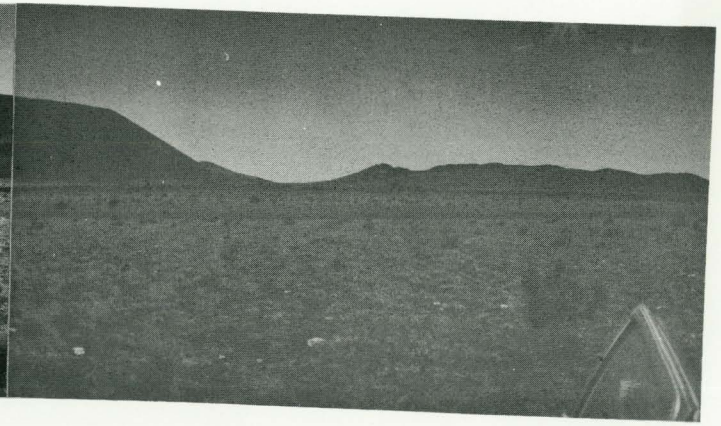

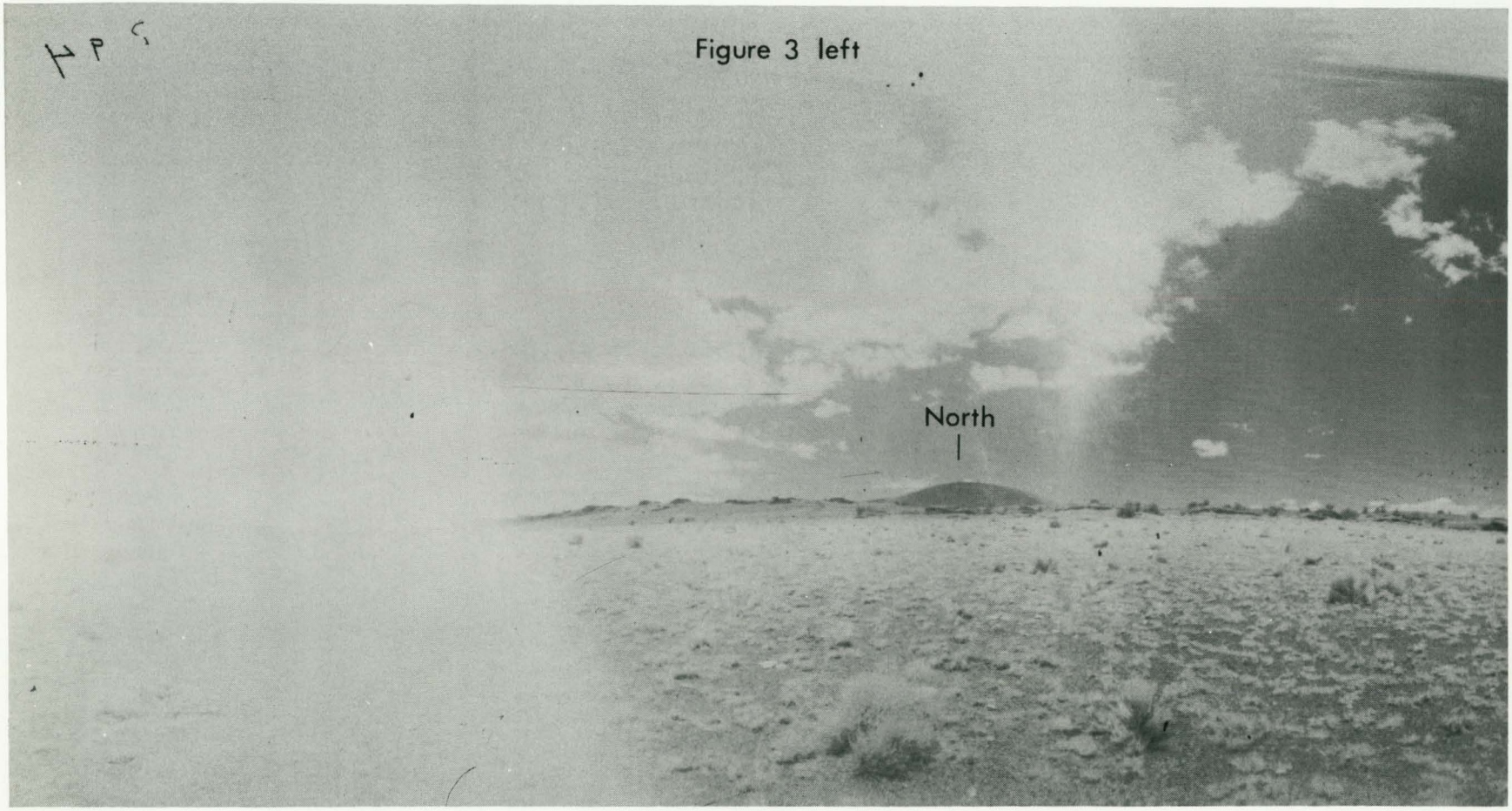
Figure 3 left
North

Figure 3 right

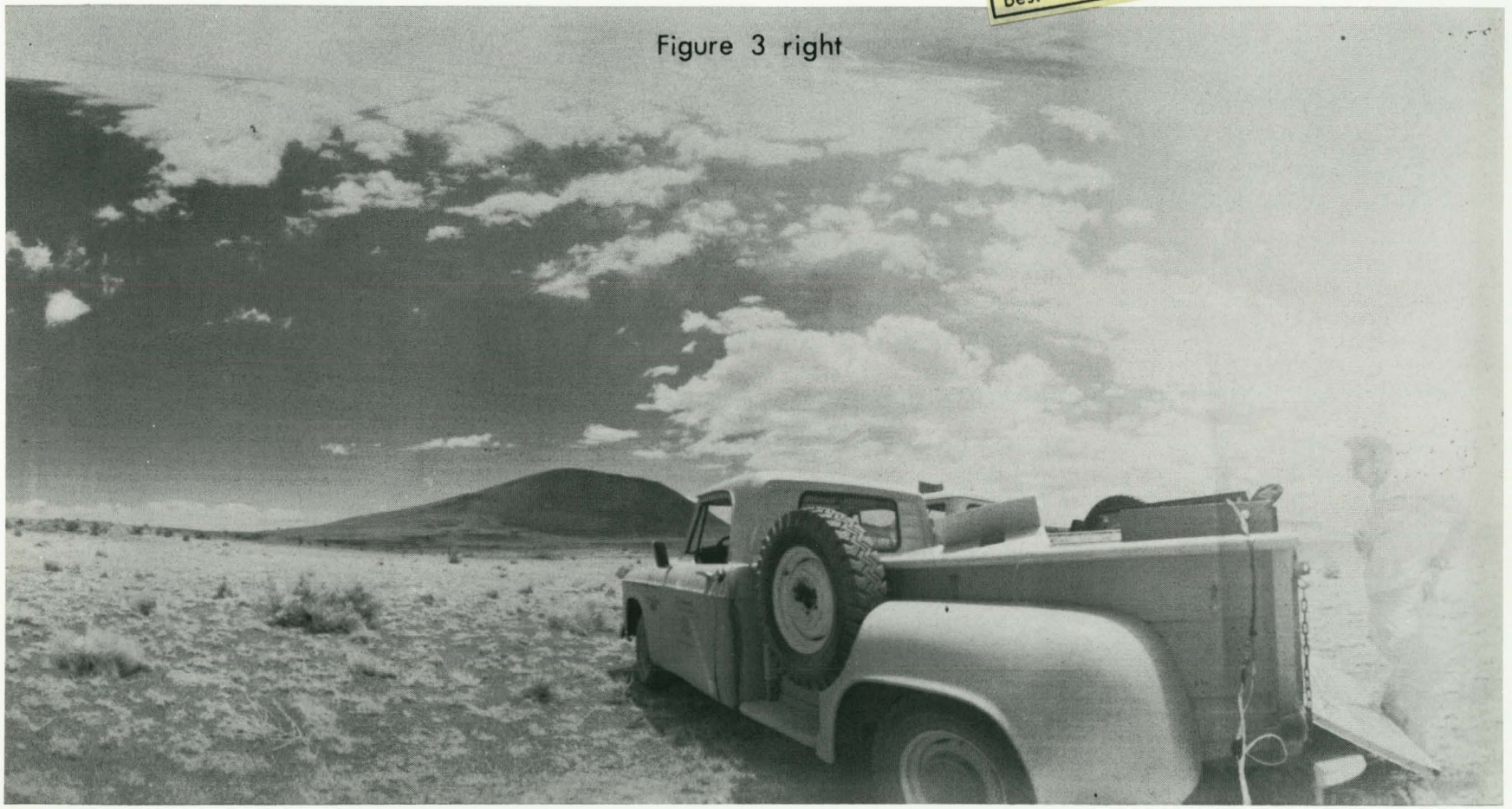

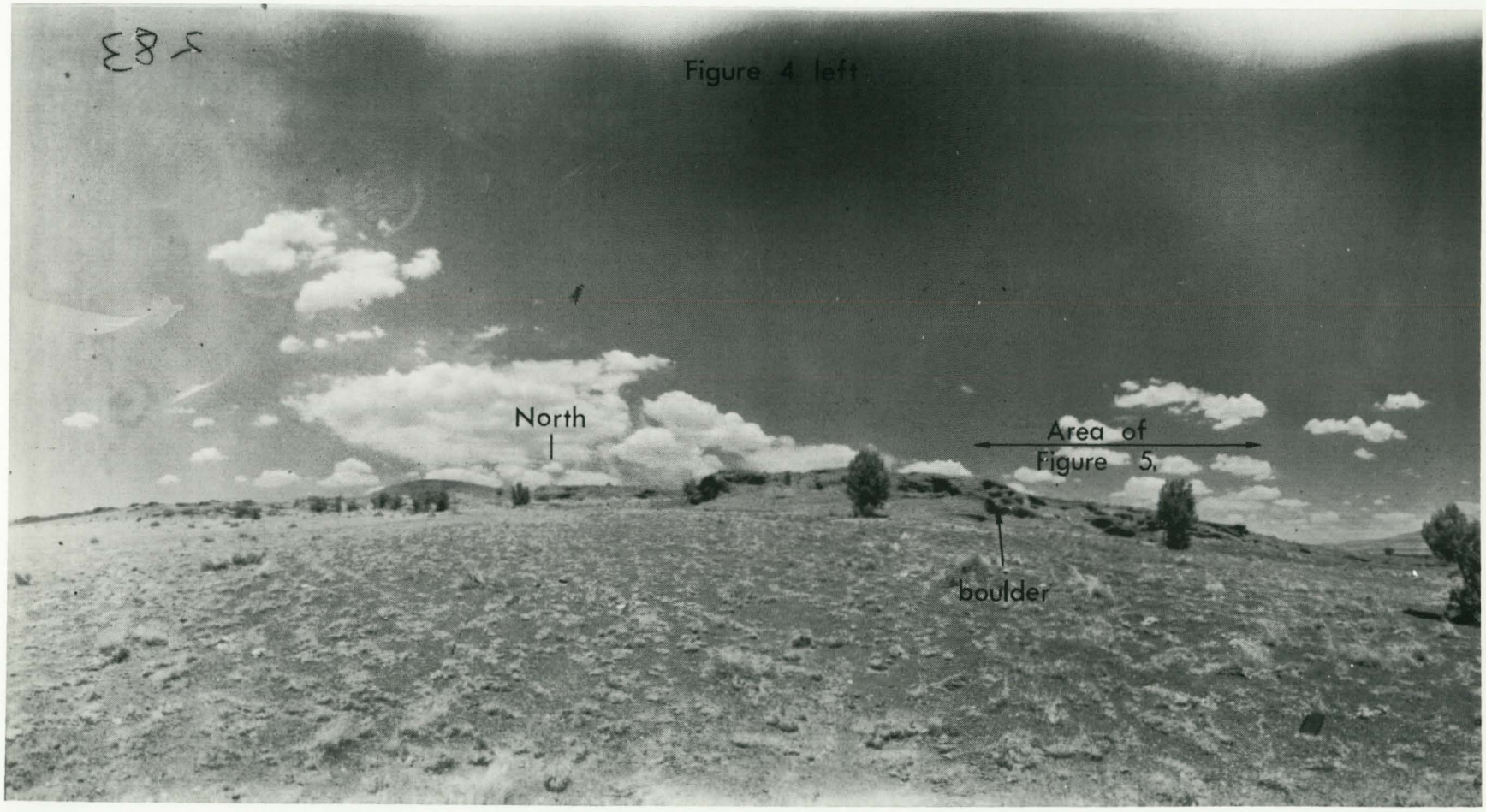
Figure 4 left
North
Area of
Figure 5.
boulder

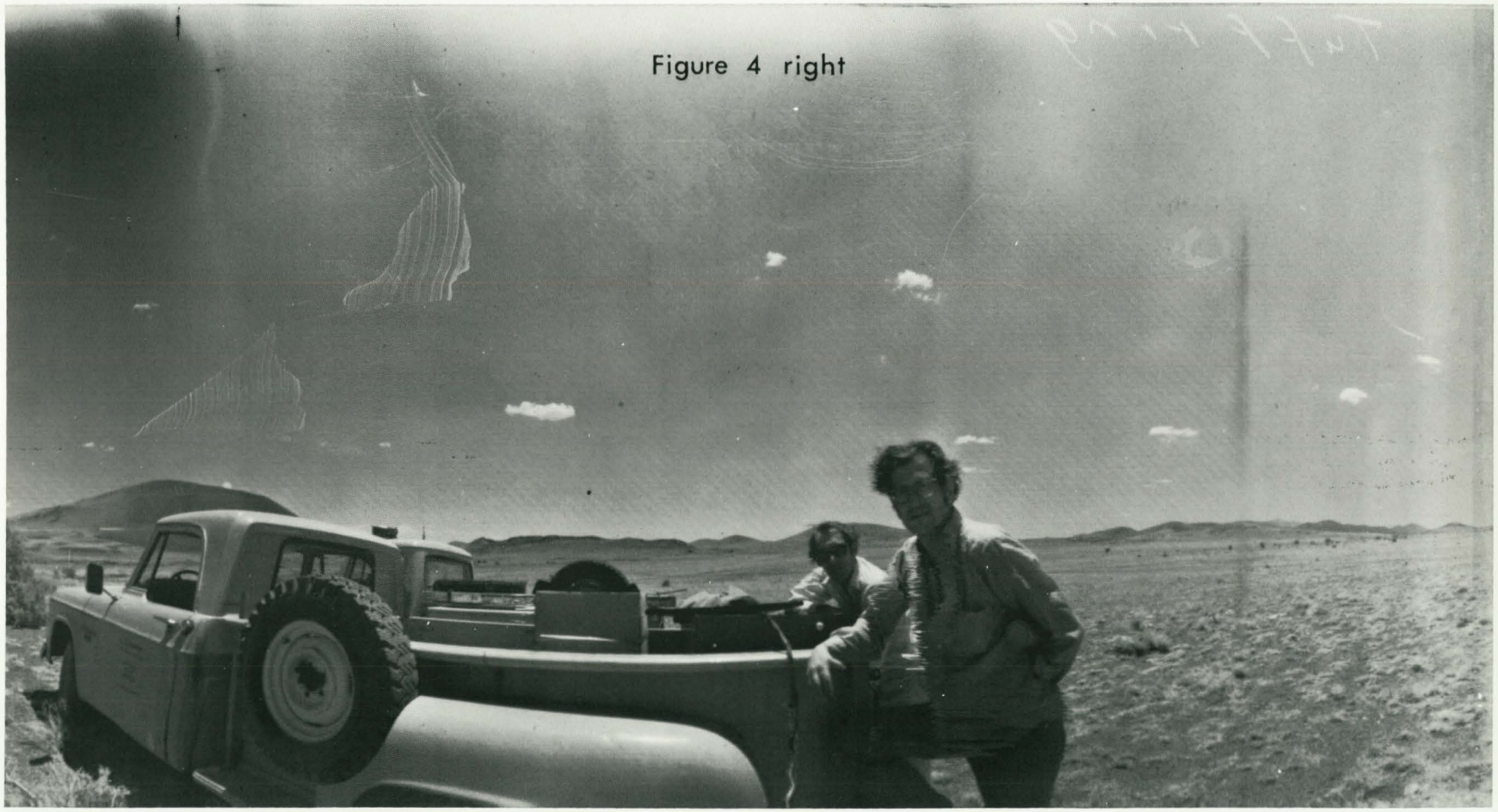

Figure 4 right

Figure 5a left

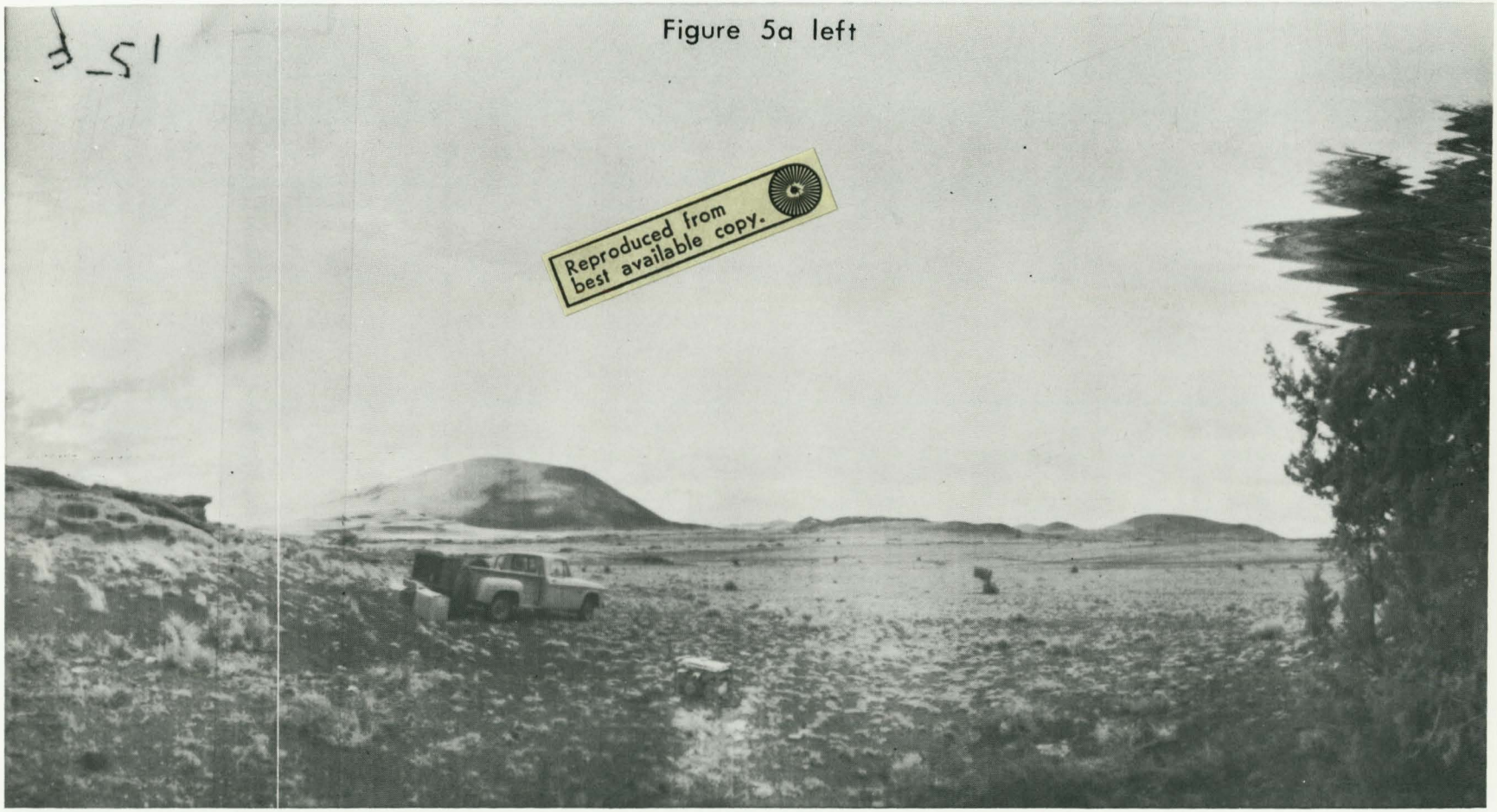

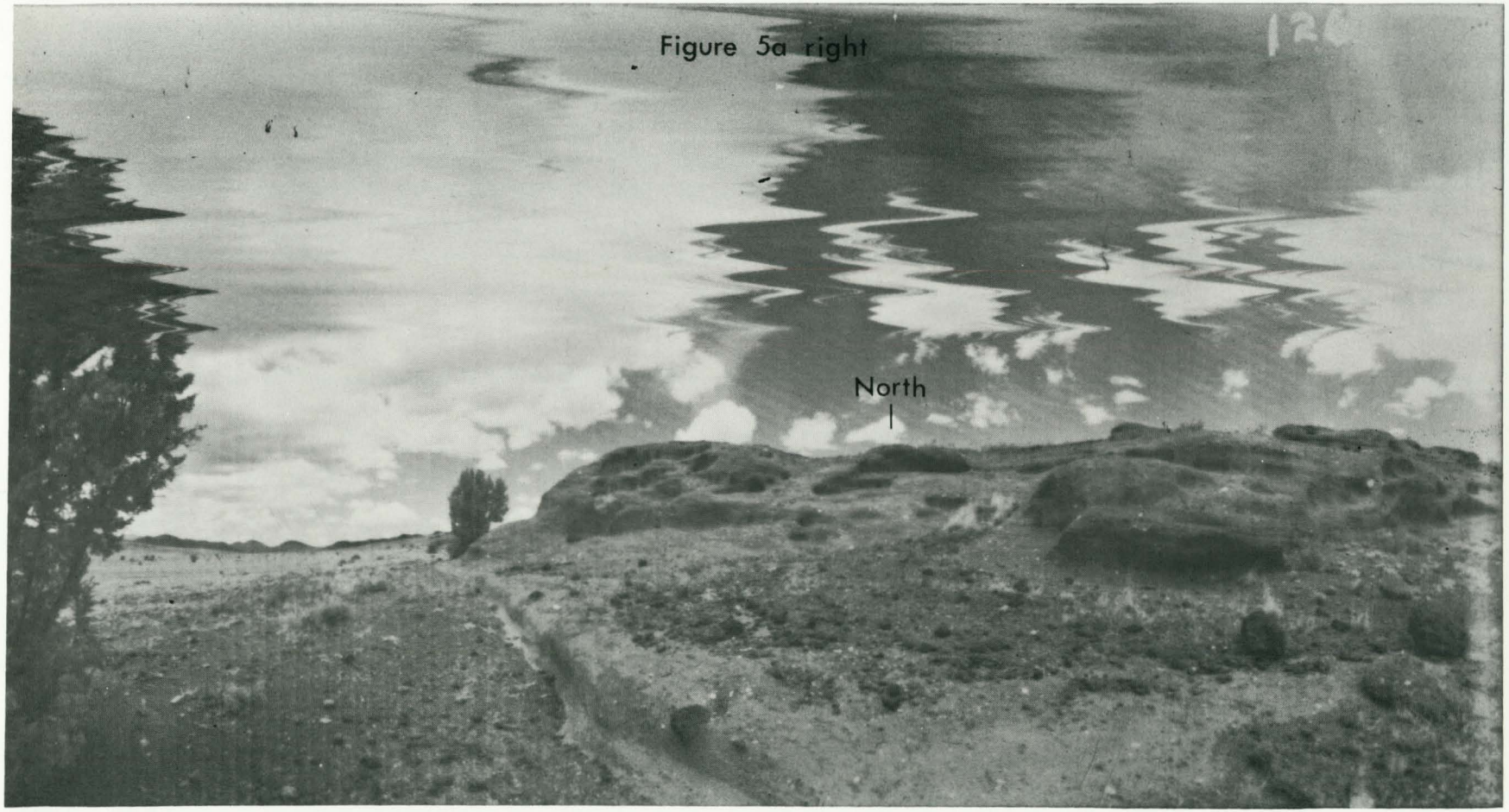
Figure 5a right
North

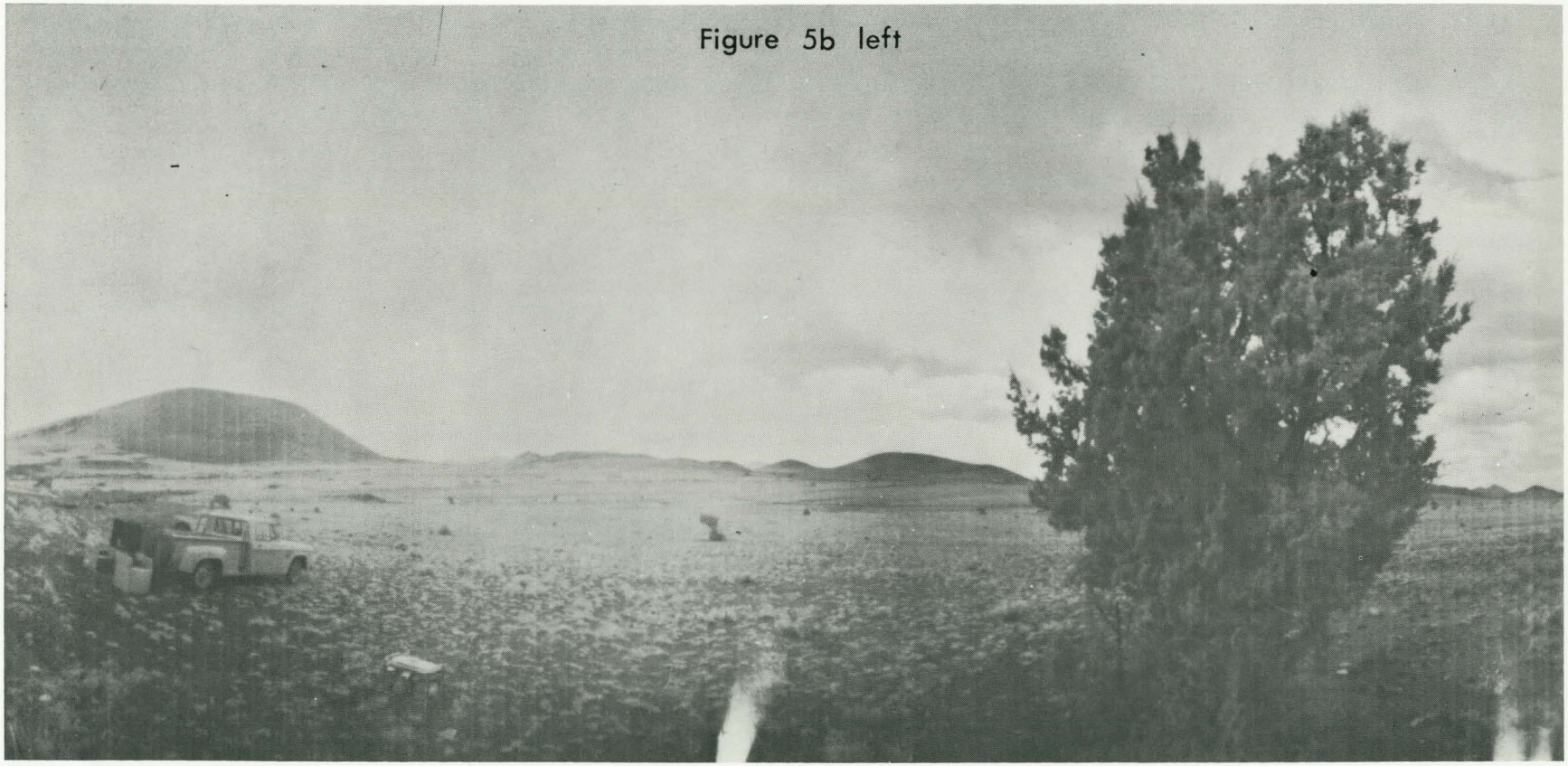

Figure 5b left

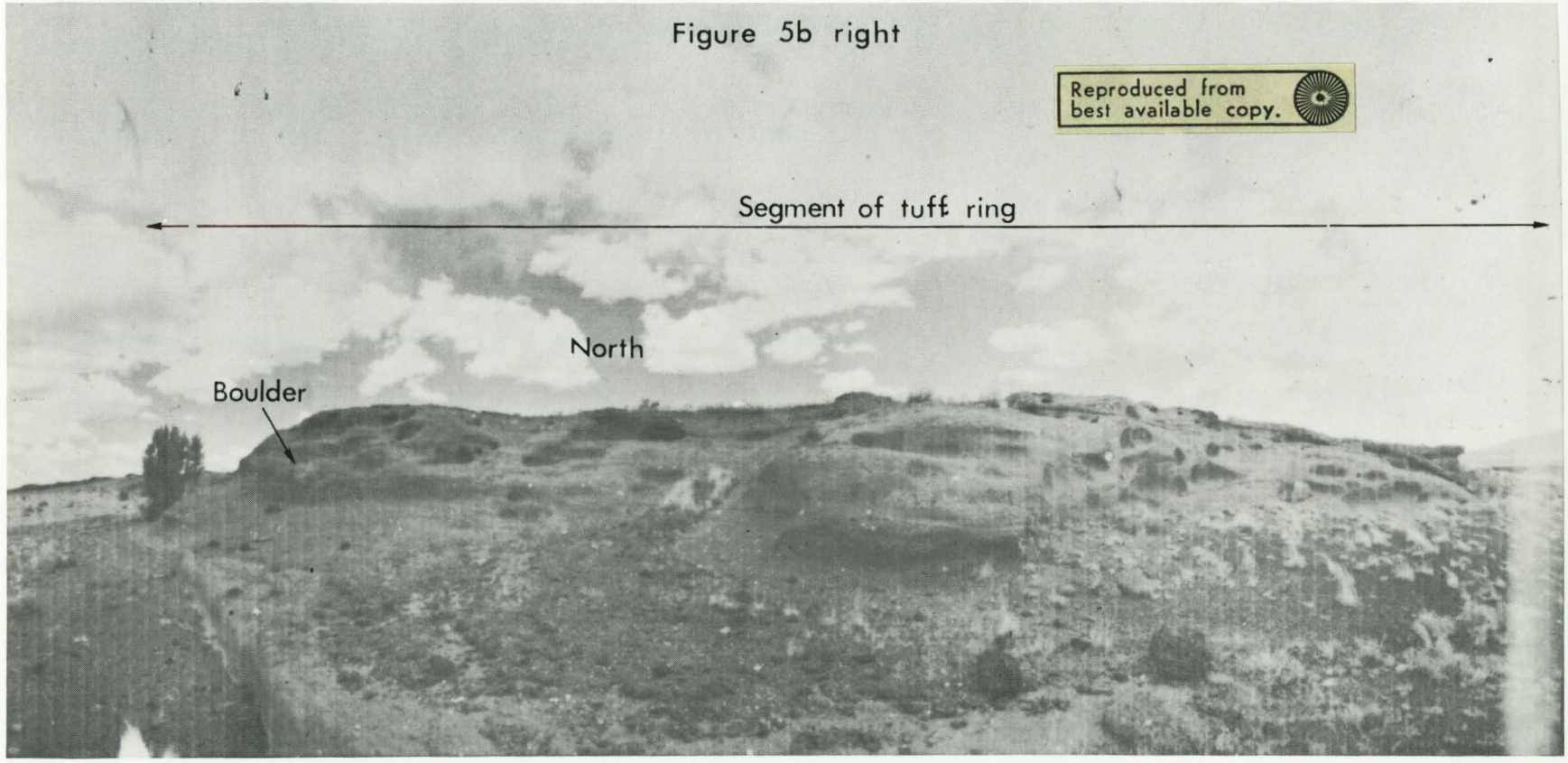
Figure 5b right
Reproduced from best available copy.
Segment of tuff ring
North
Boulder

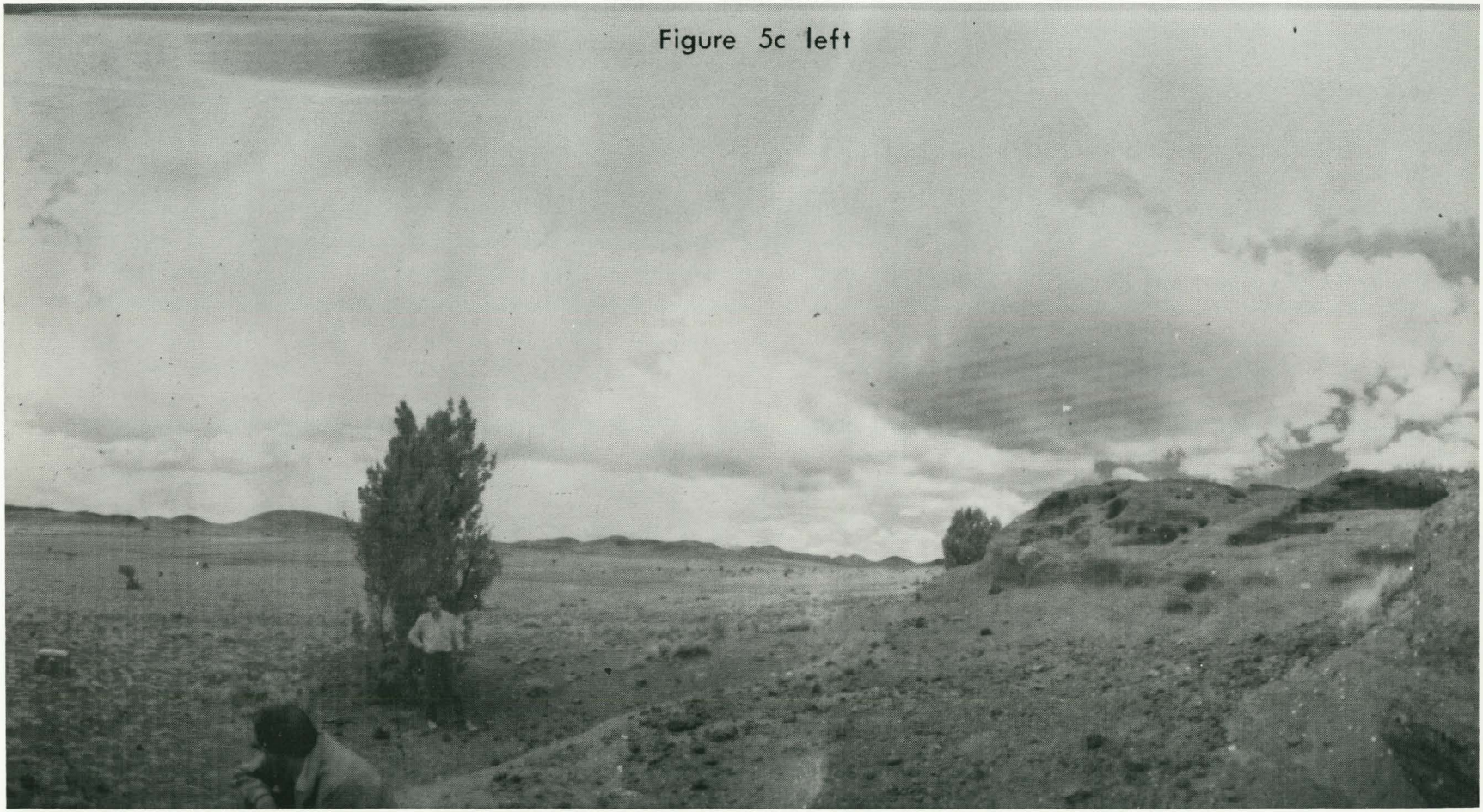

Figure 5c left

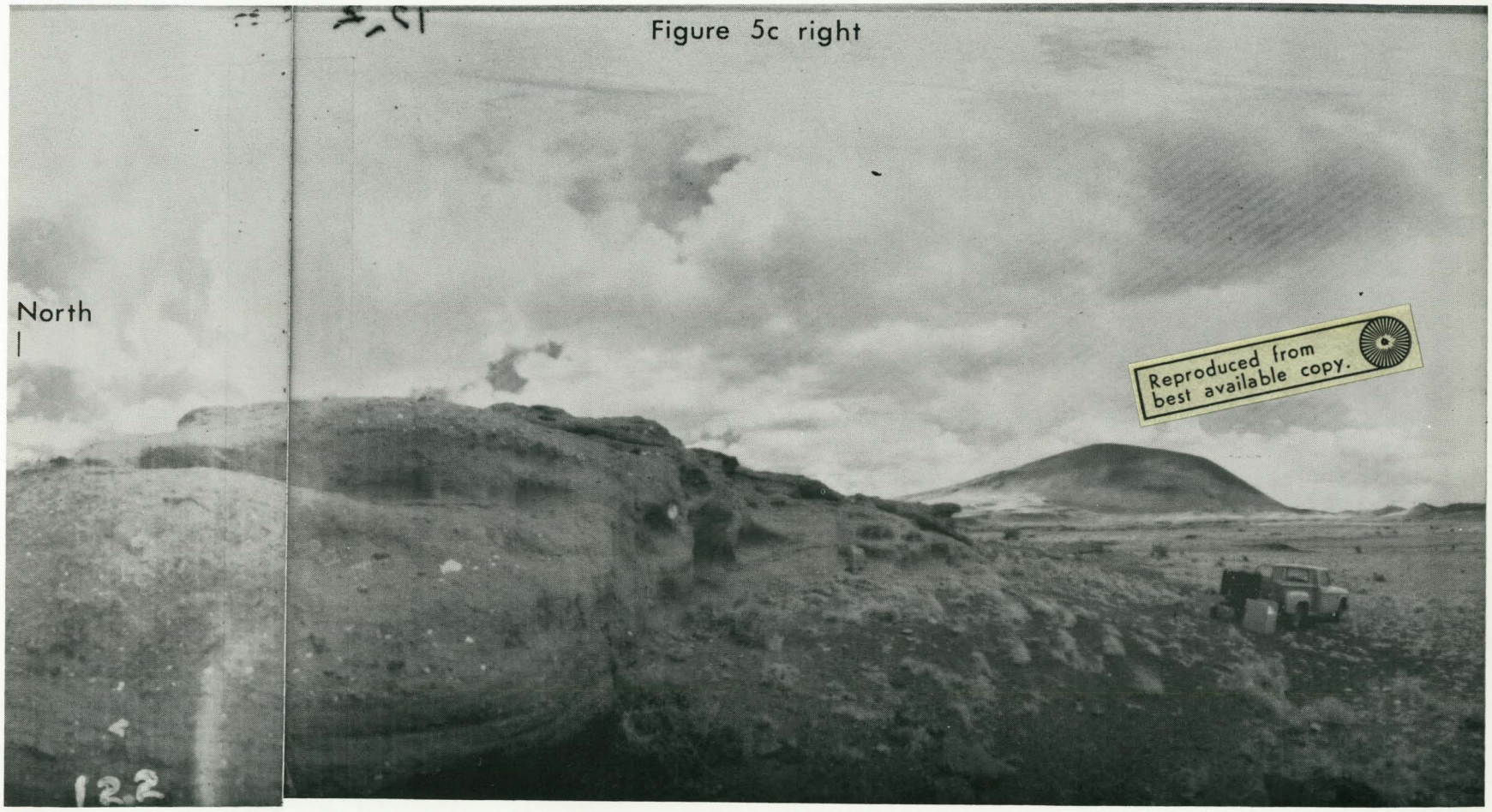
Figure 5c right
North
Reproduced from
best available copy.
122

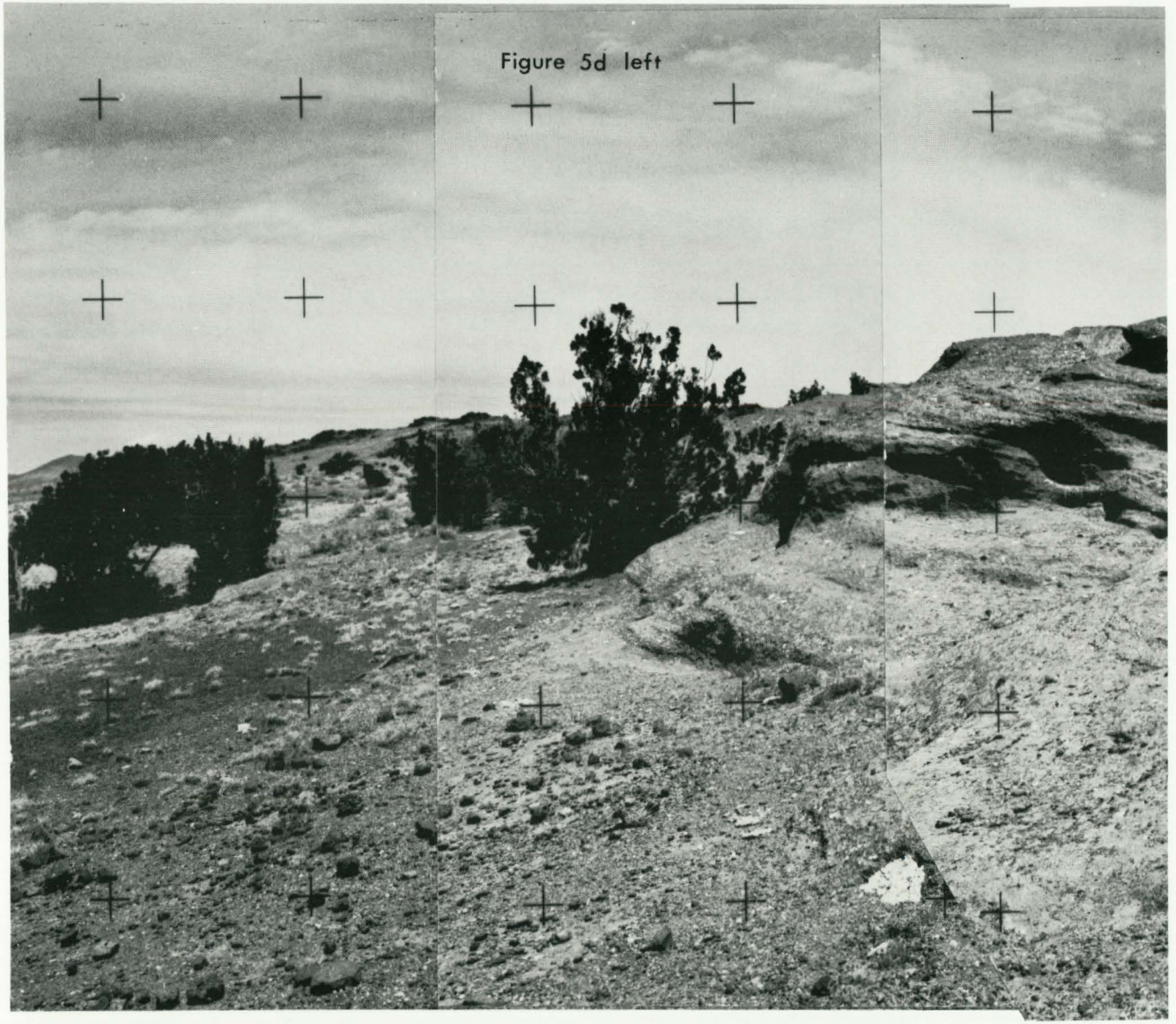
Figure 5d left


Figure 5d right

Figure 5e

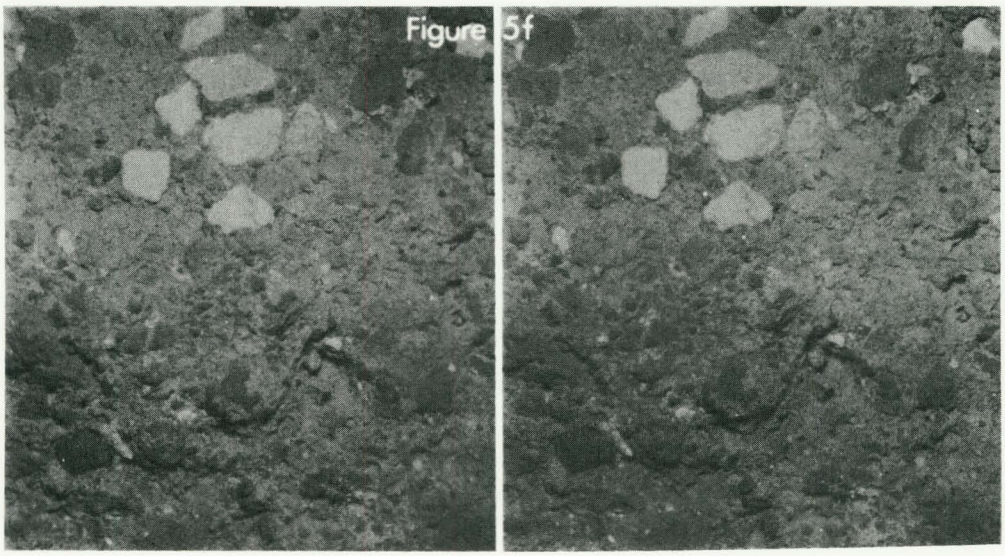
Figure 5f


Figure 6a left
North


Figure 6a right

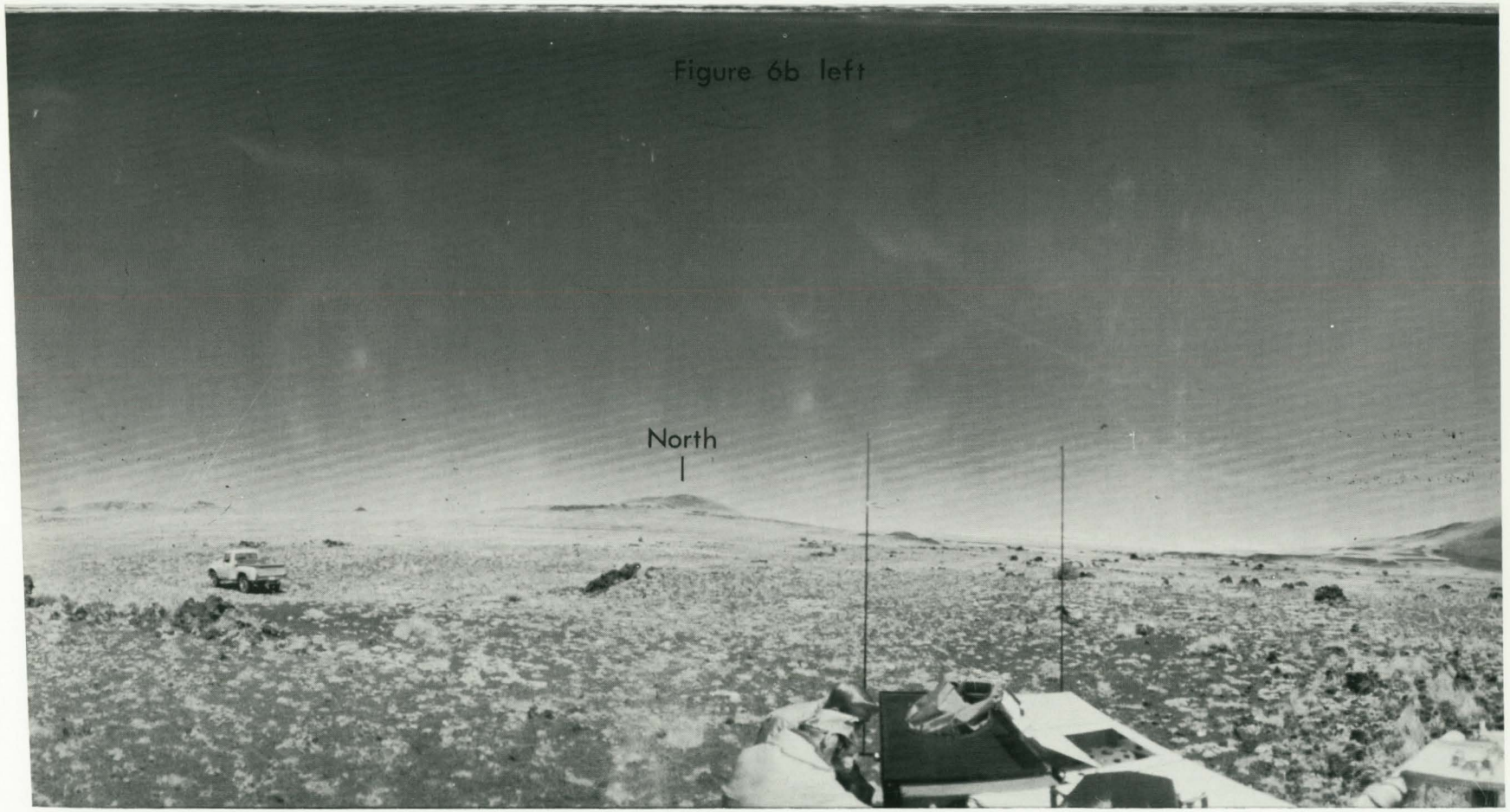
Figure 6b left
North

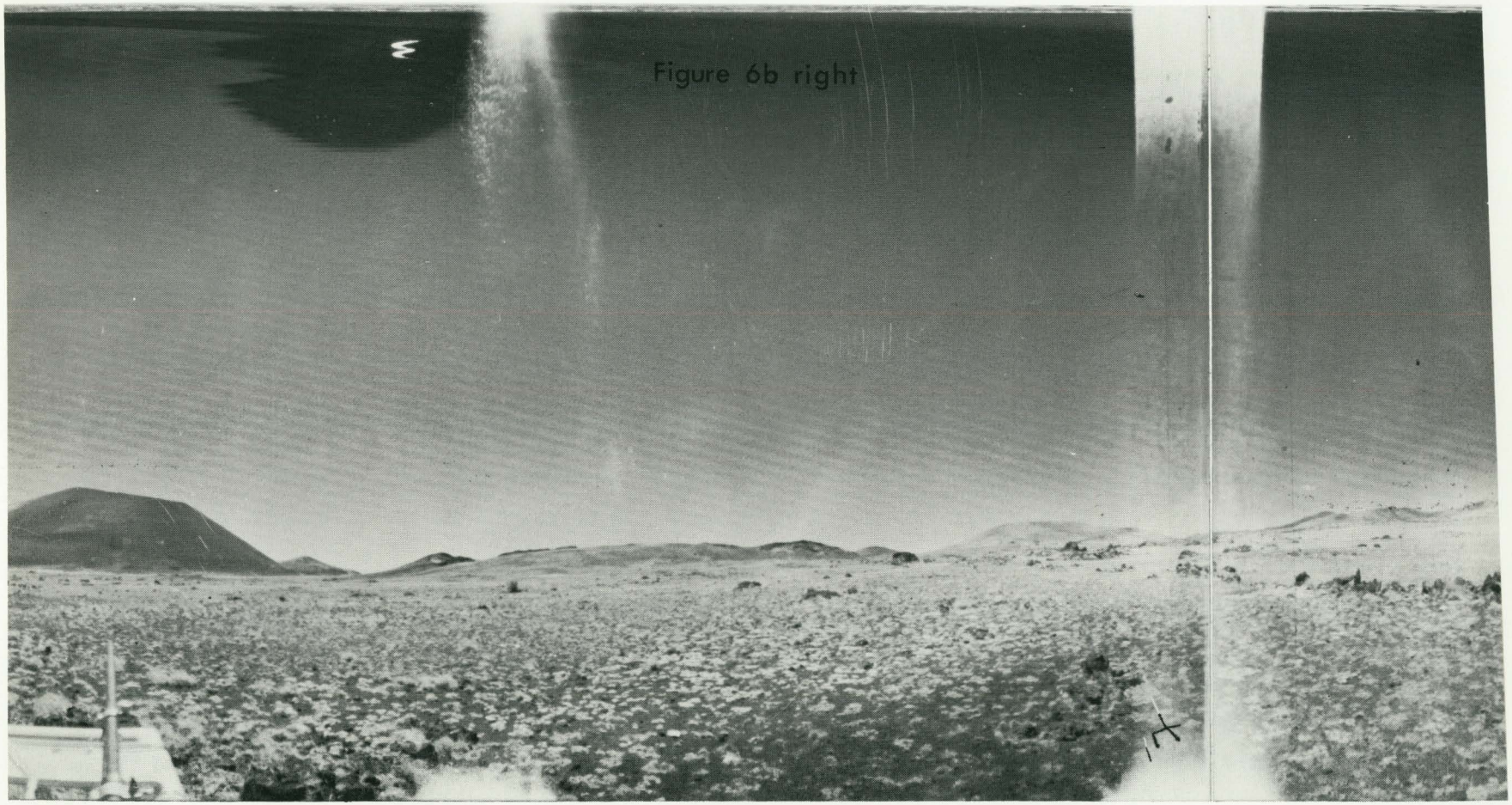
Figure 6b right

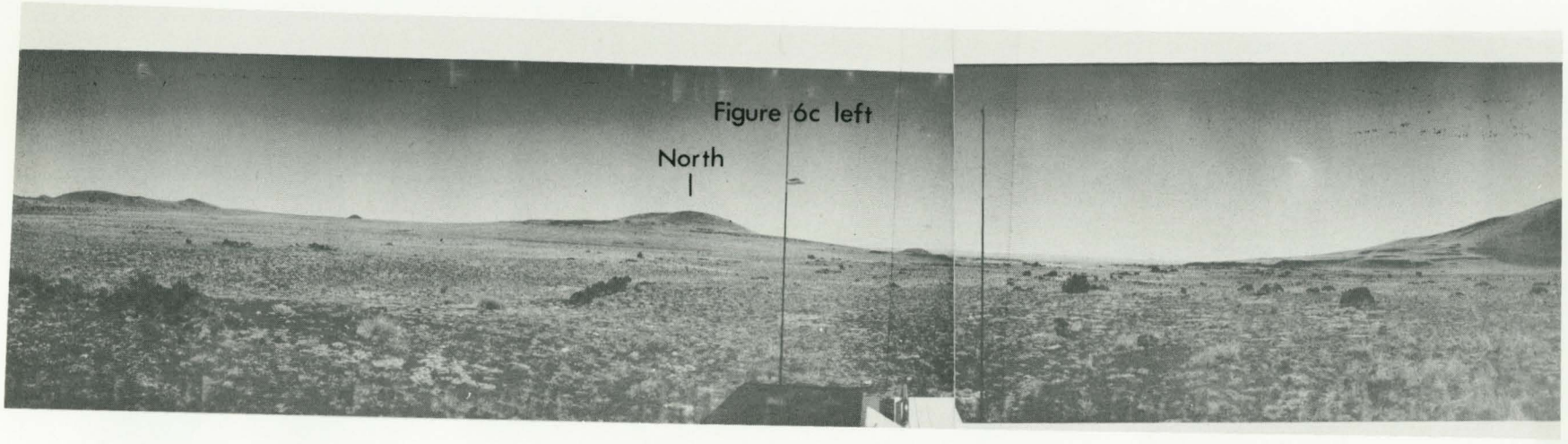

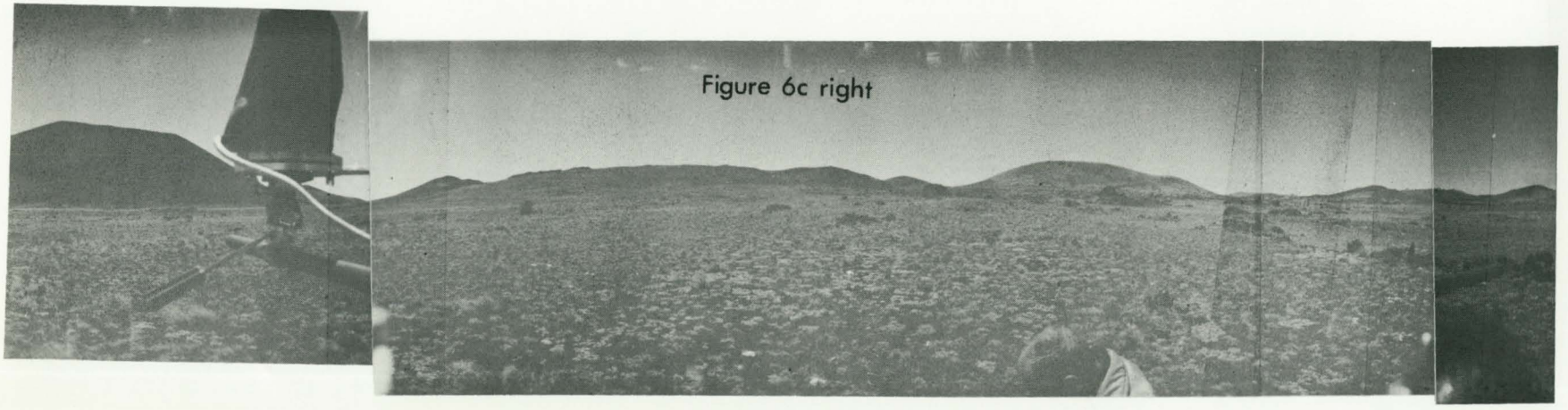

Figure 7a

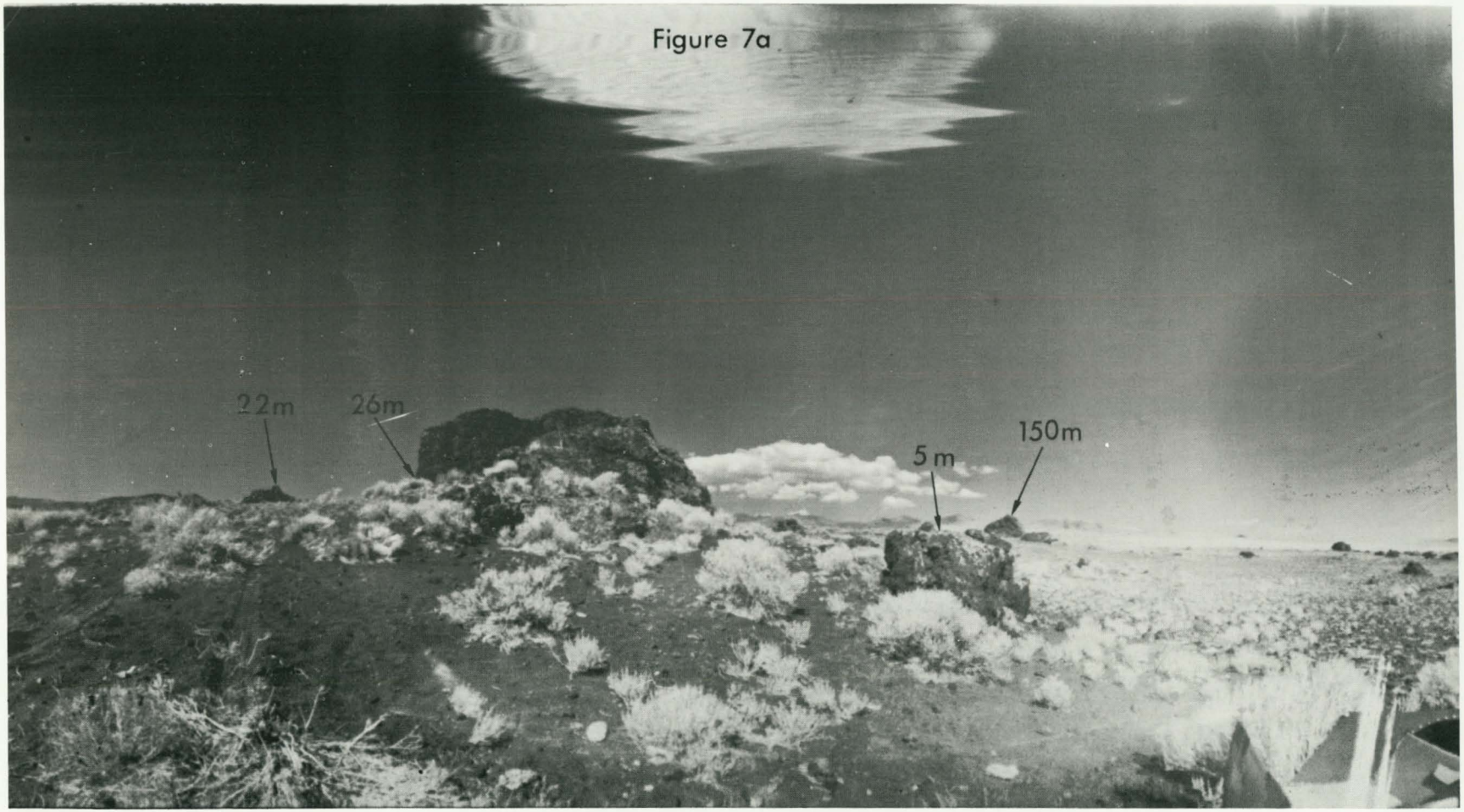

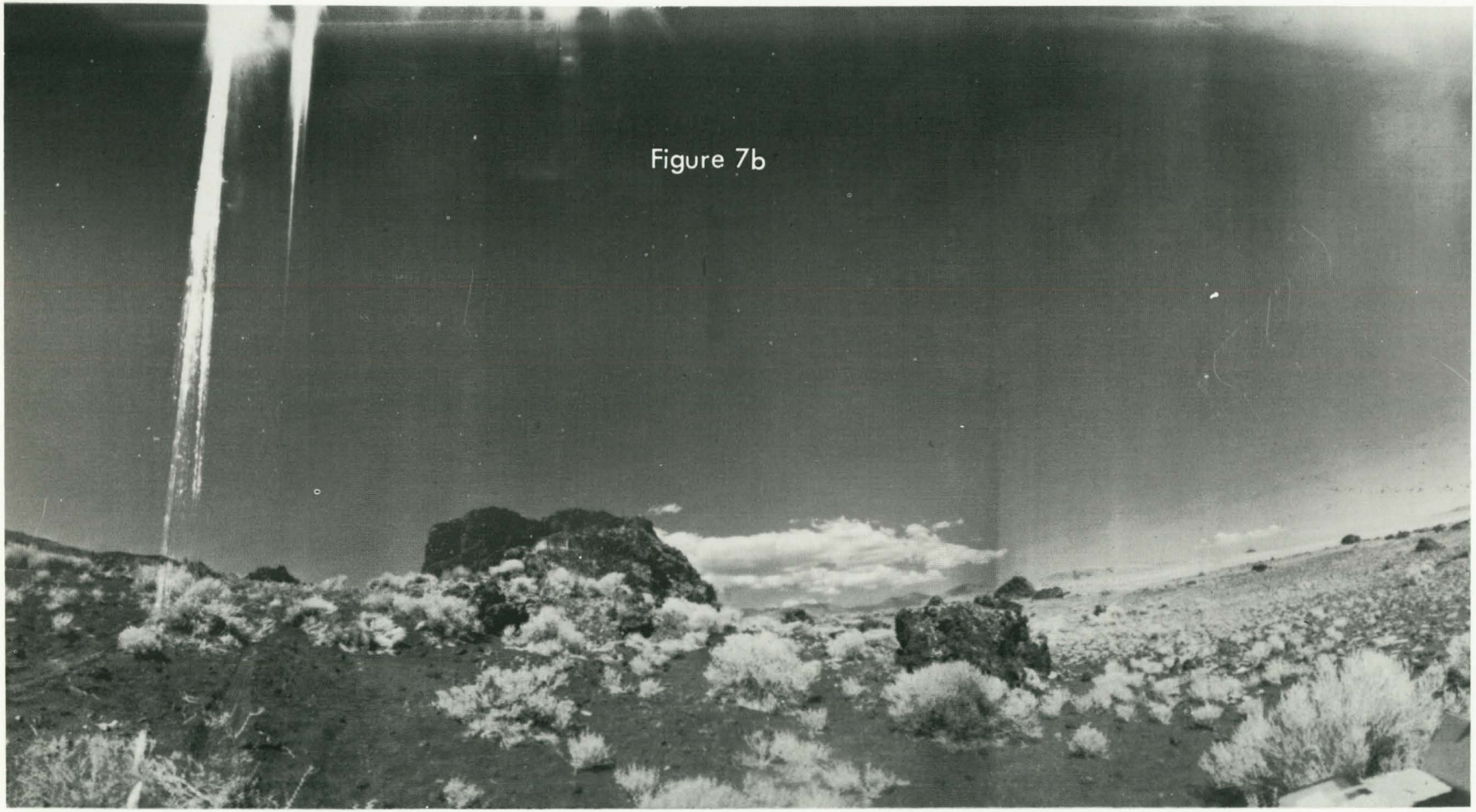
Figure 7b

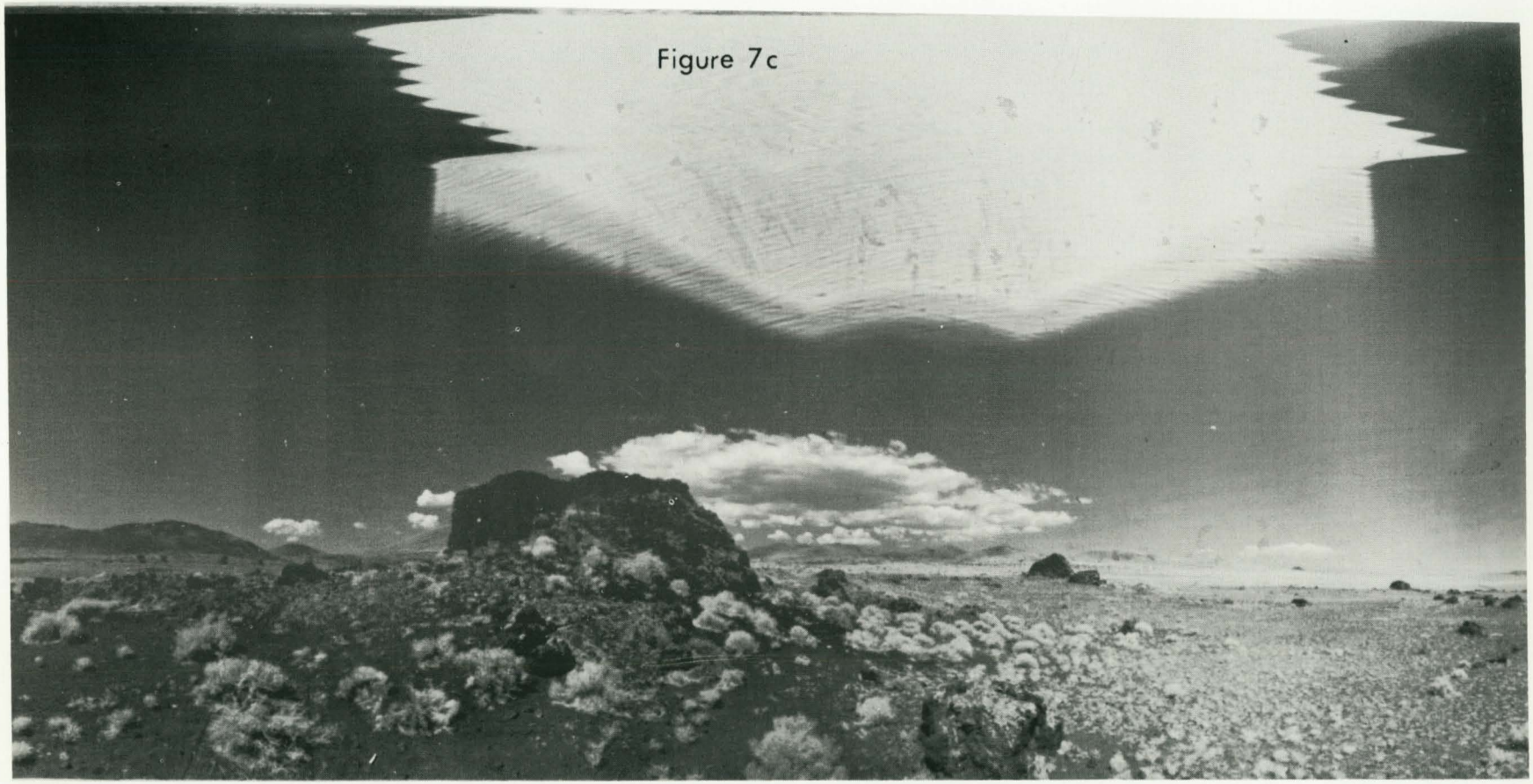

Figure 7c

Figure 7d

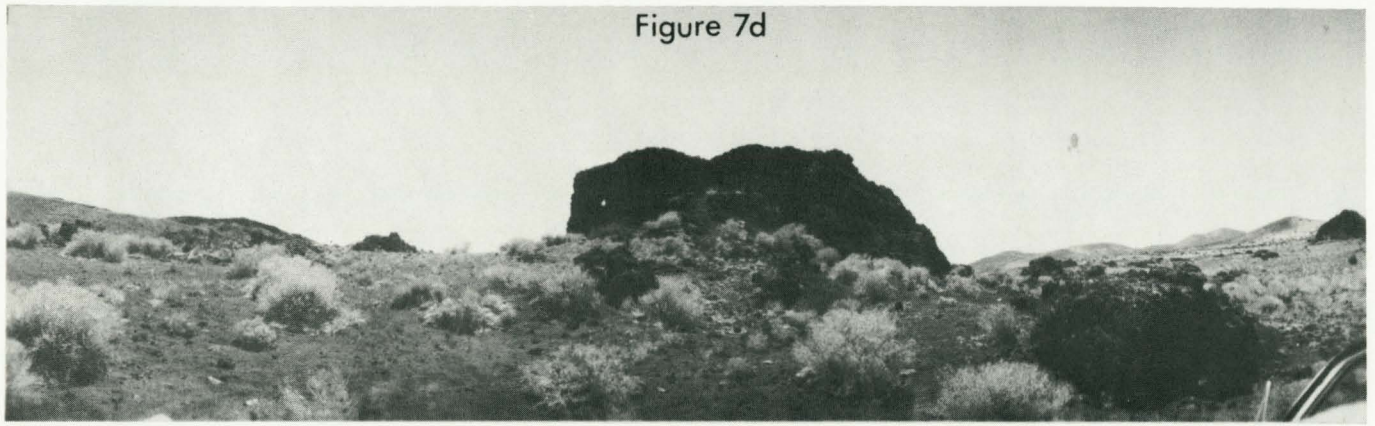

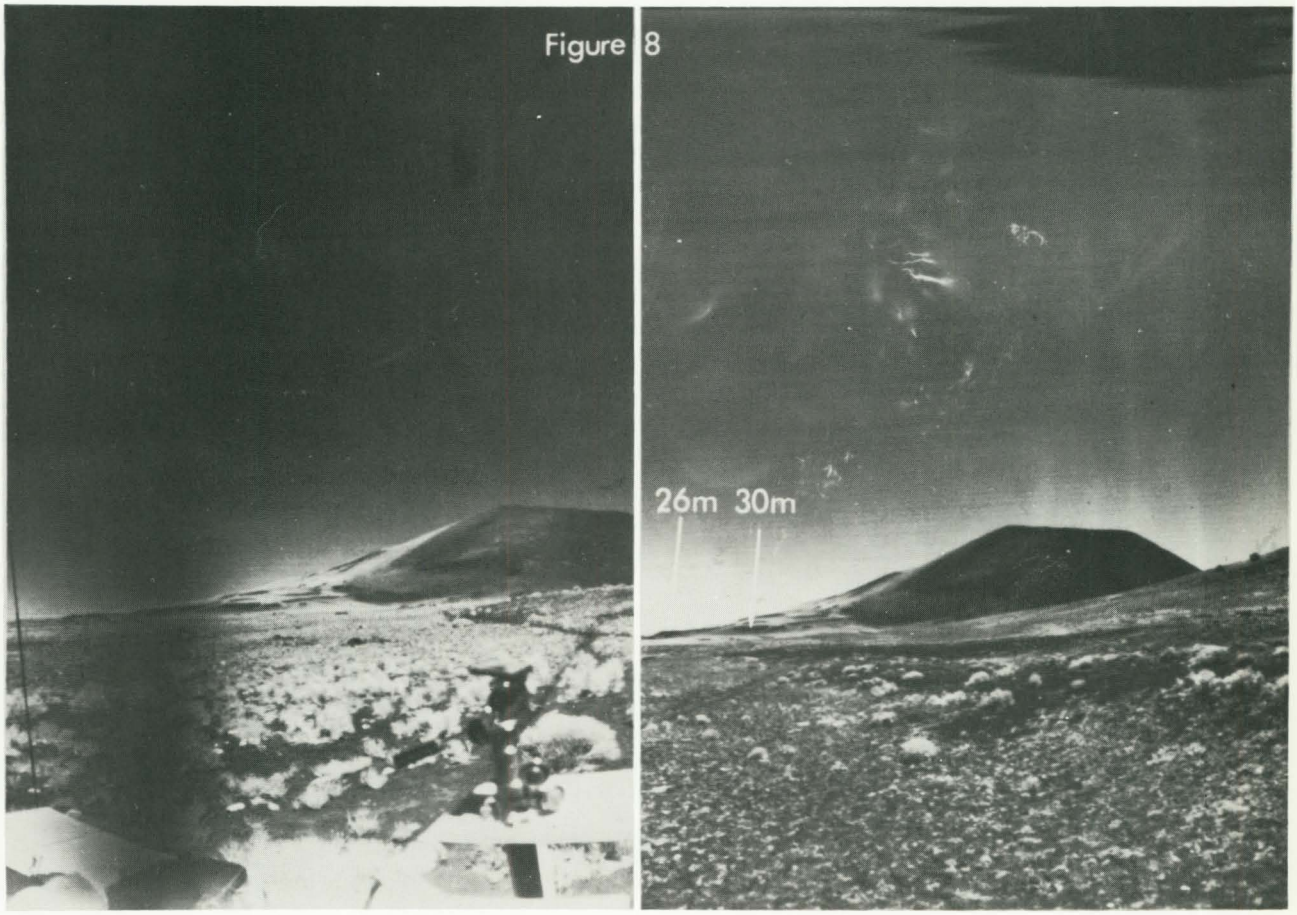
Figure 8
26m 30m

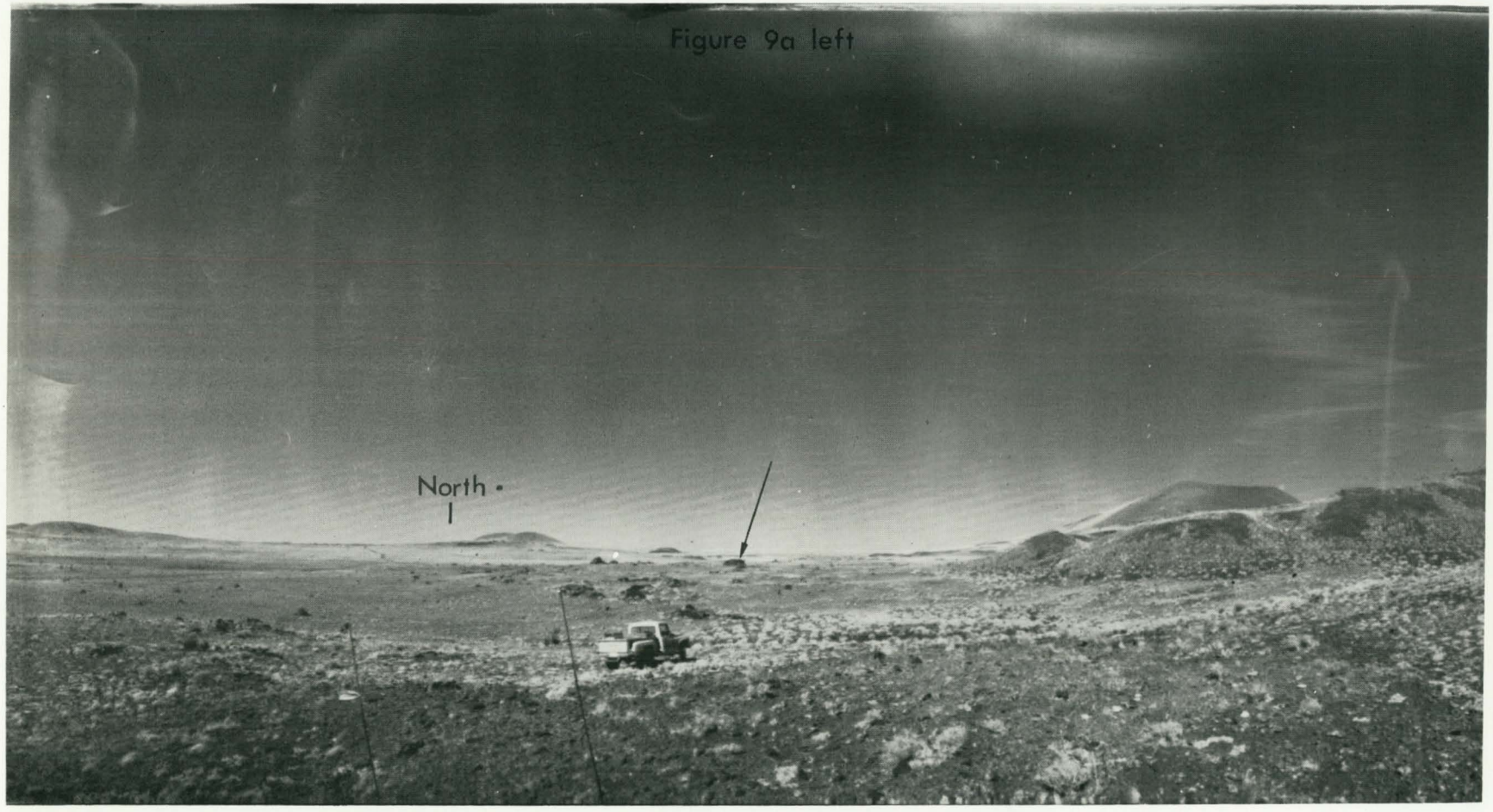
Figure 9a left
North

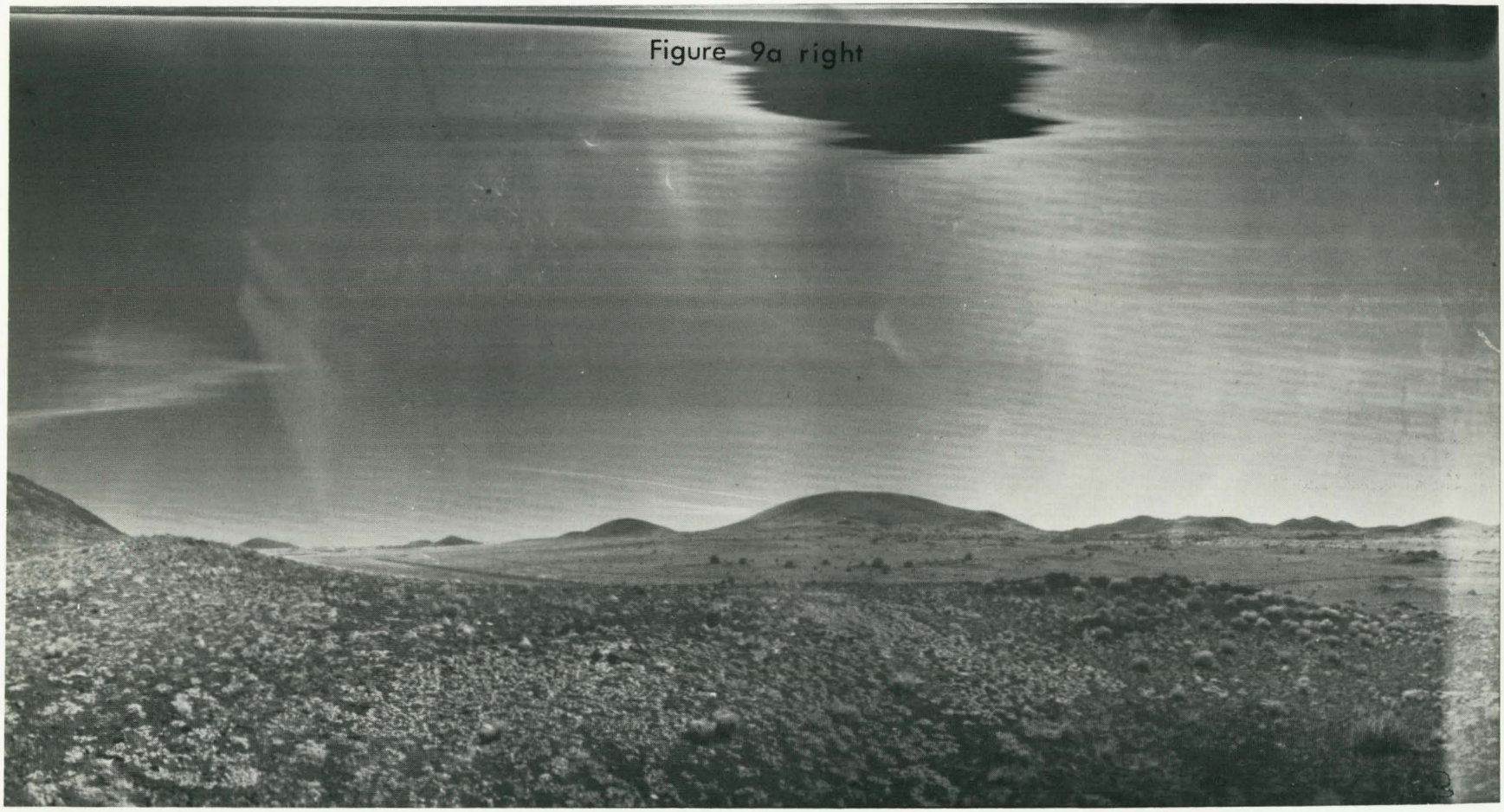

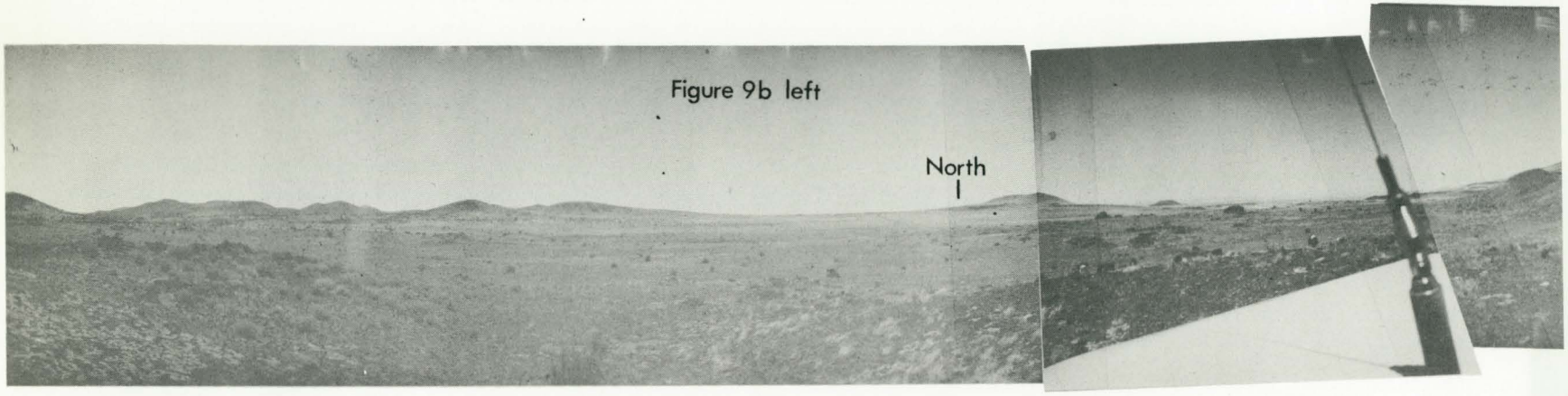
Figure 9b left
North

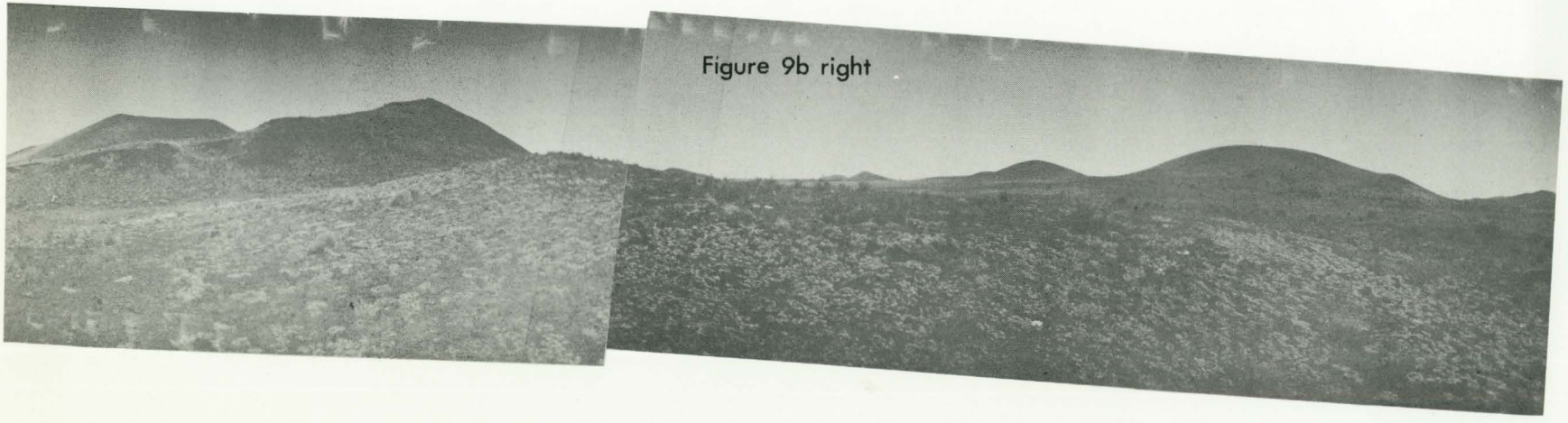
Figure 9b right

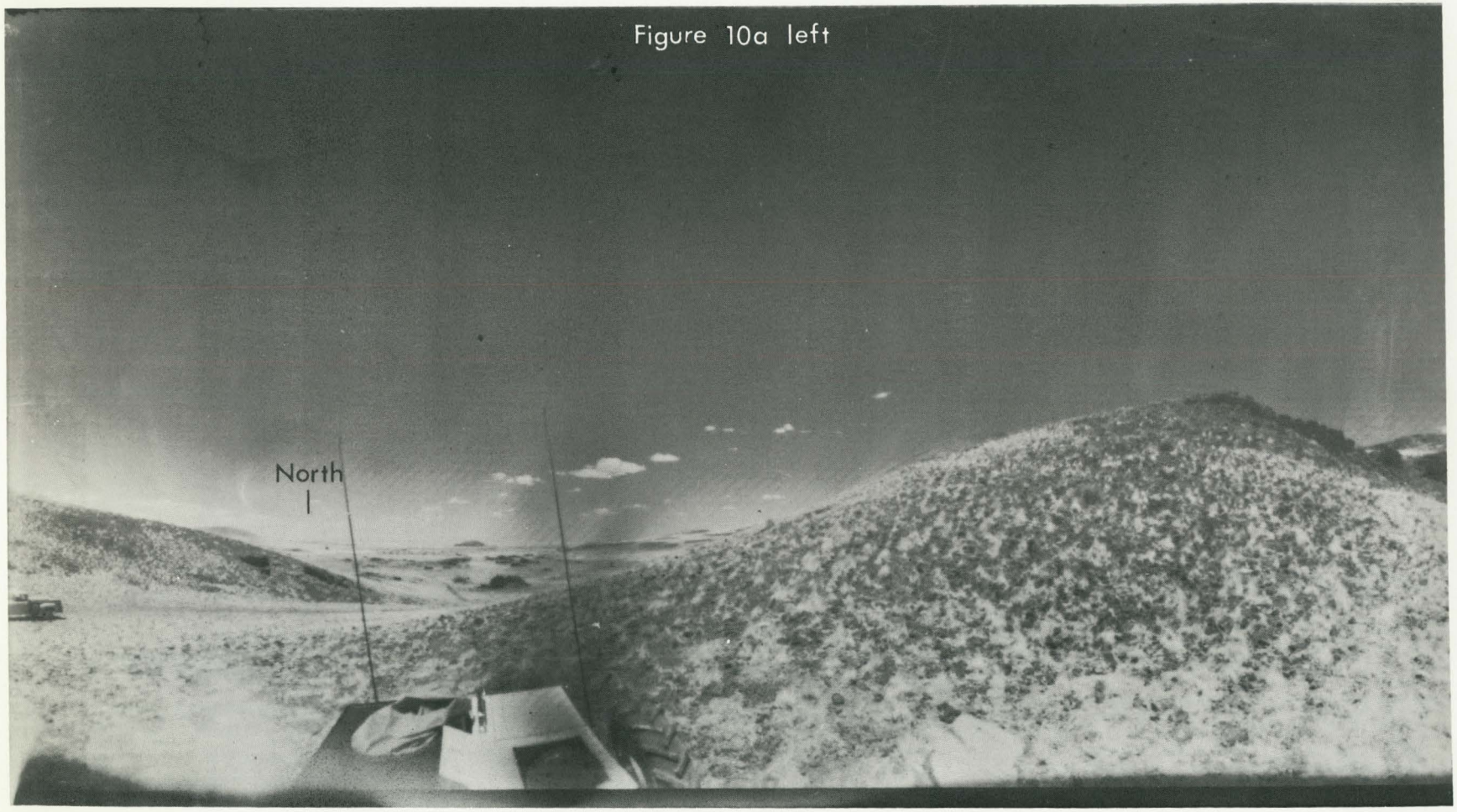
Figure 10a left
North

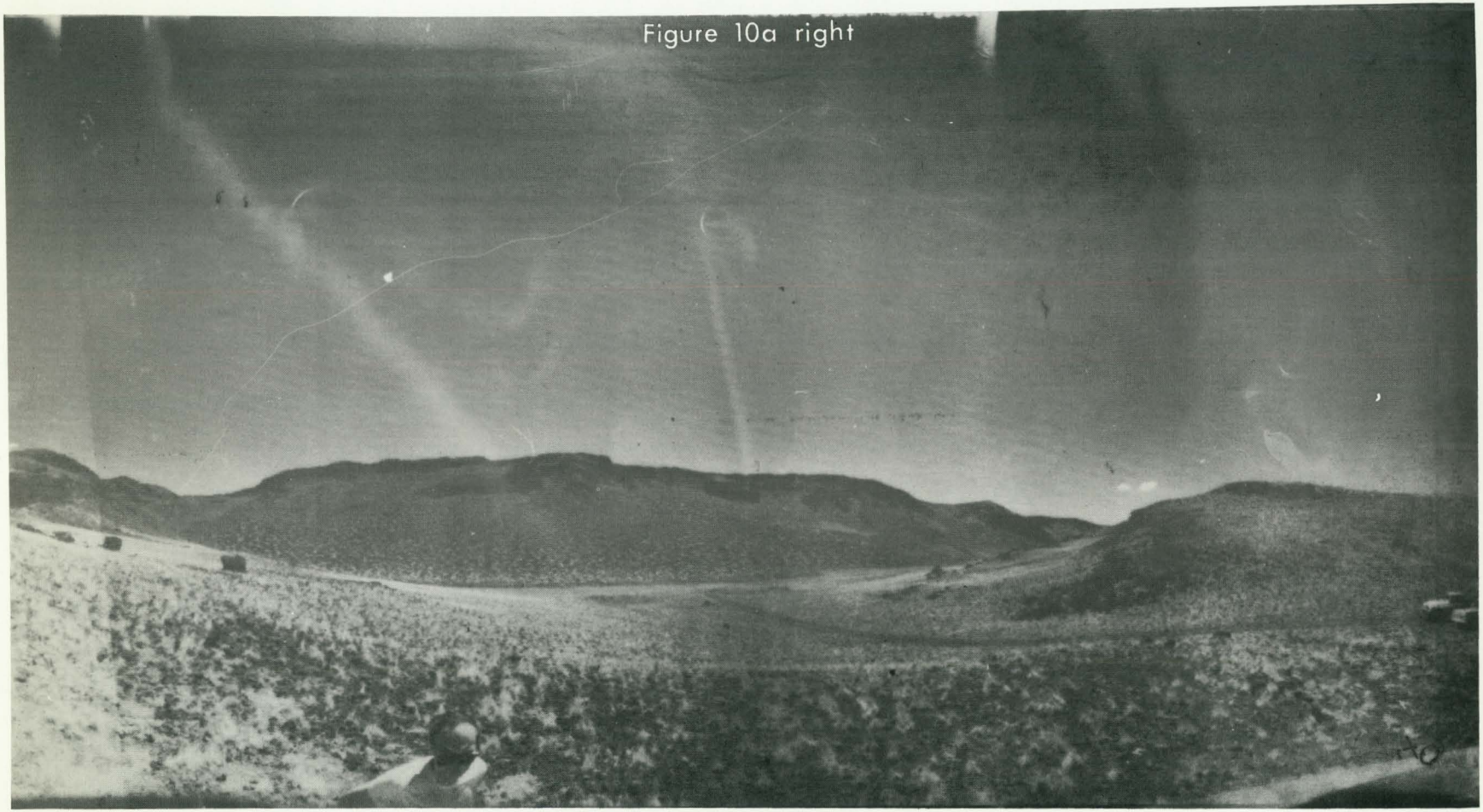
Figure 10a right

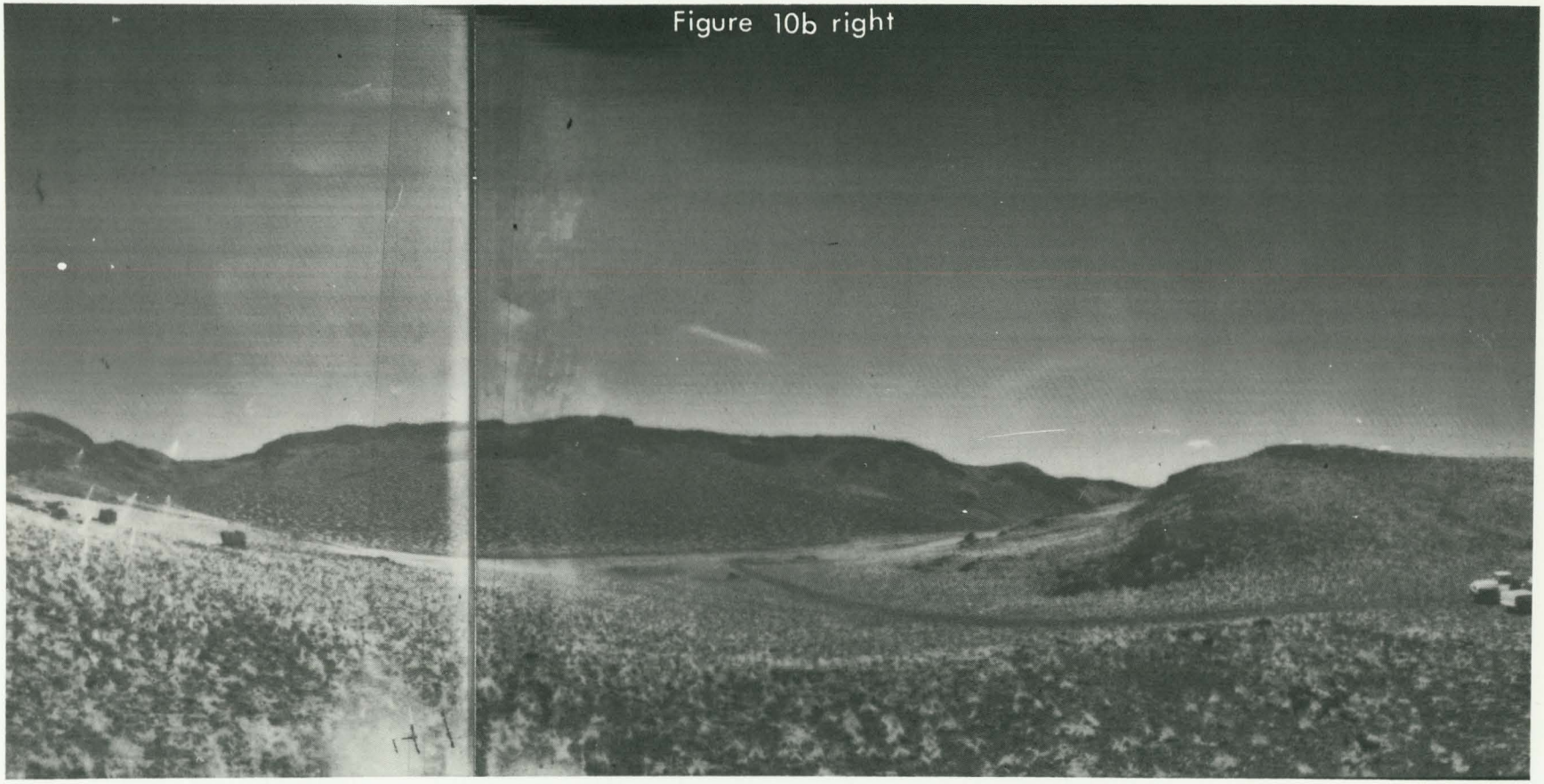
Figure 10b right

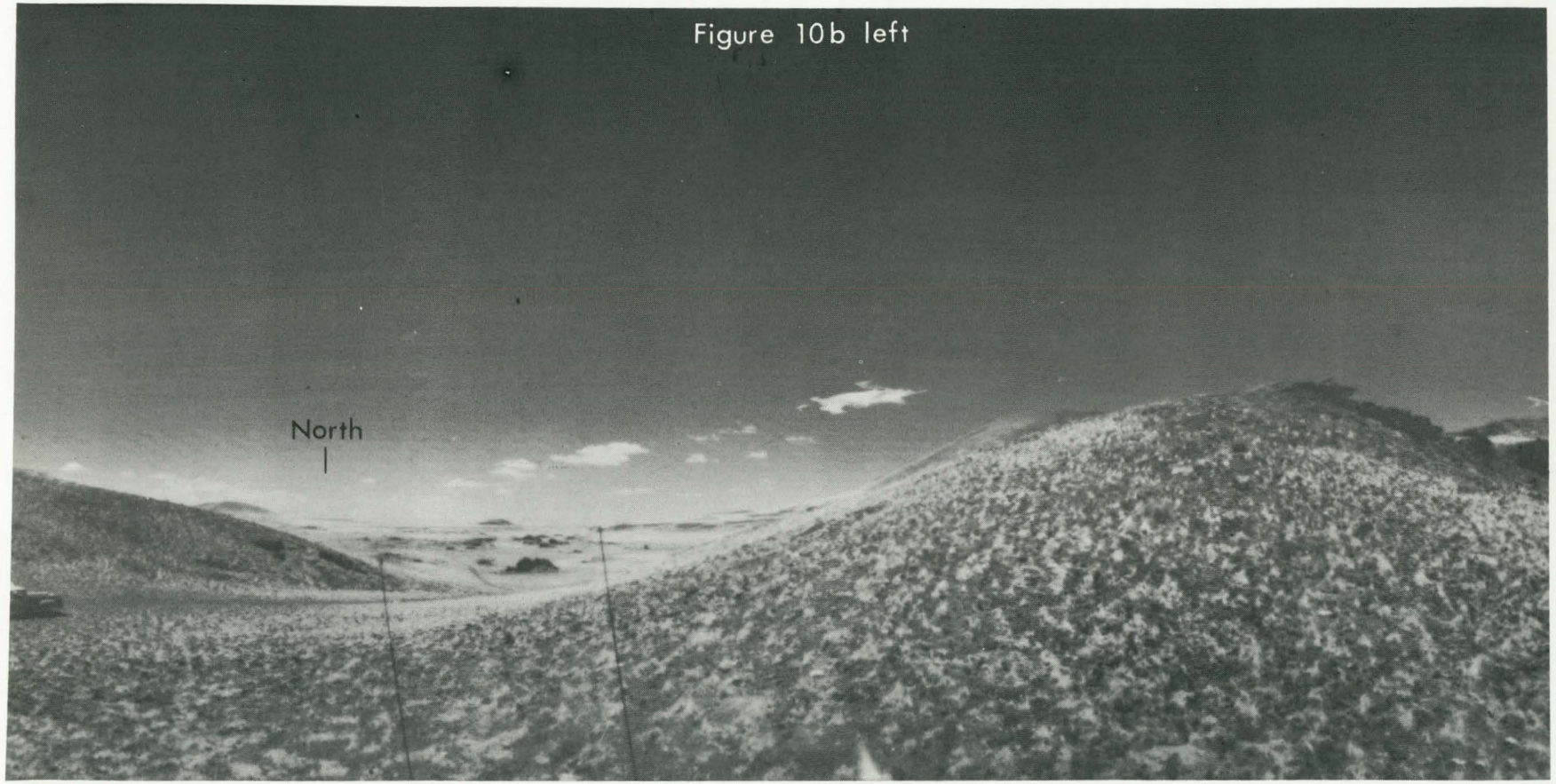
Figure 10b left
North

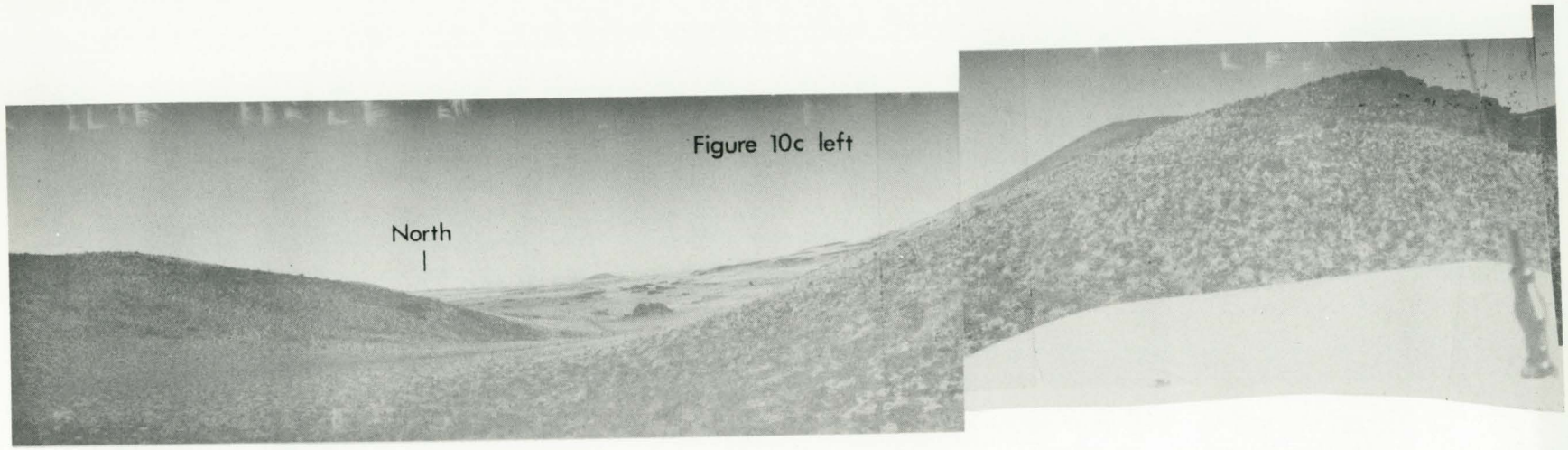

Figure 10c left

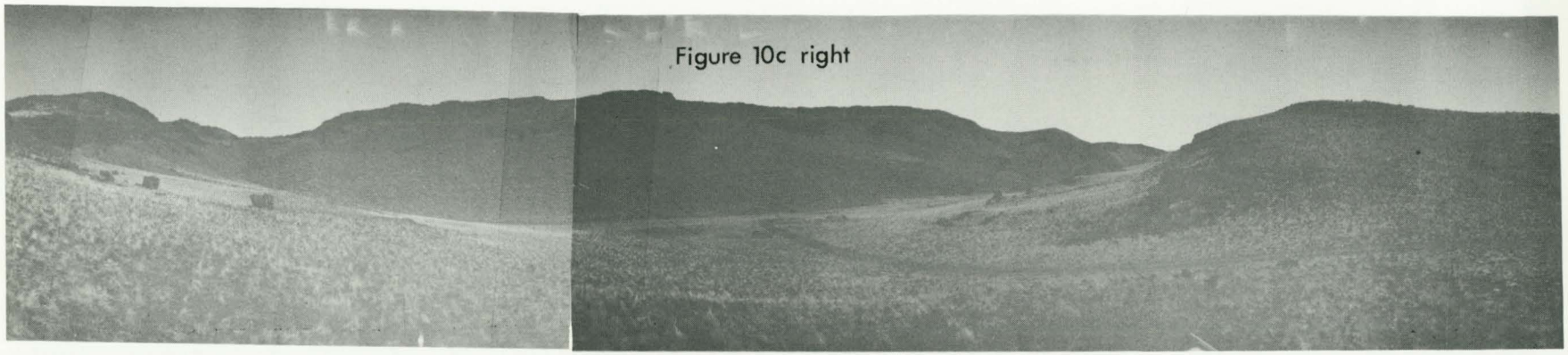

Figure 10c right

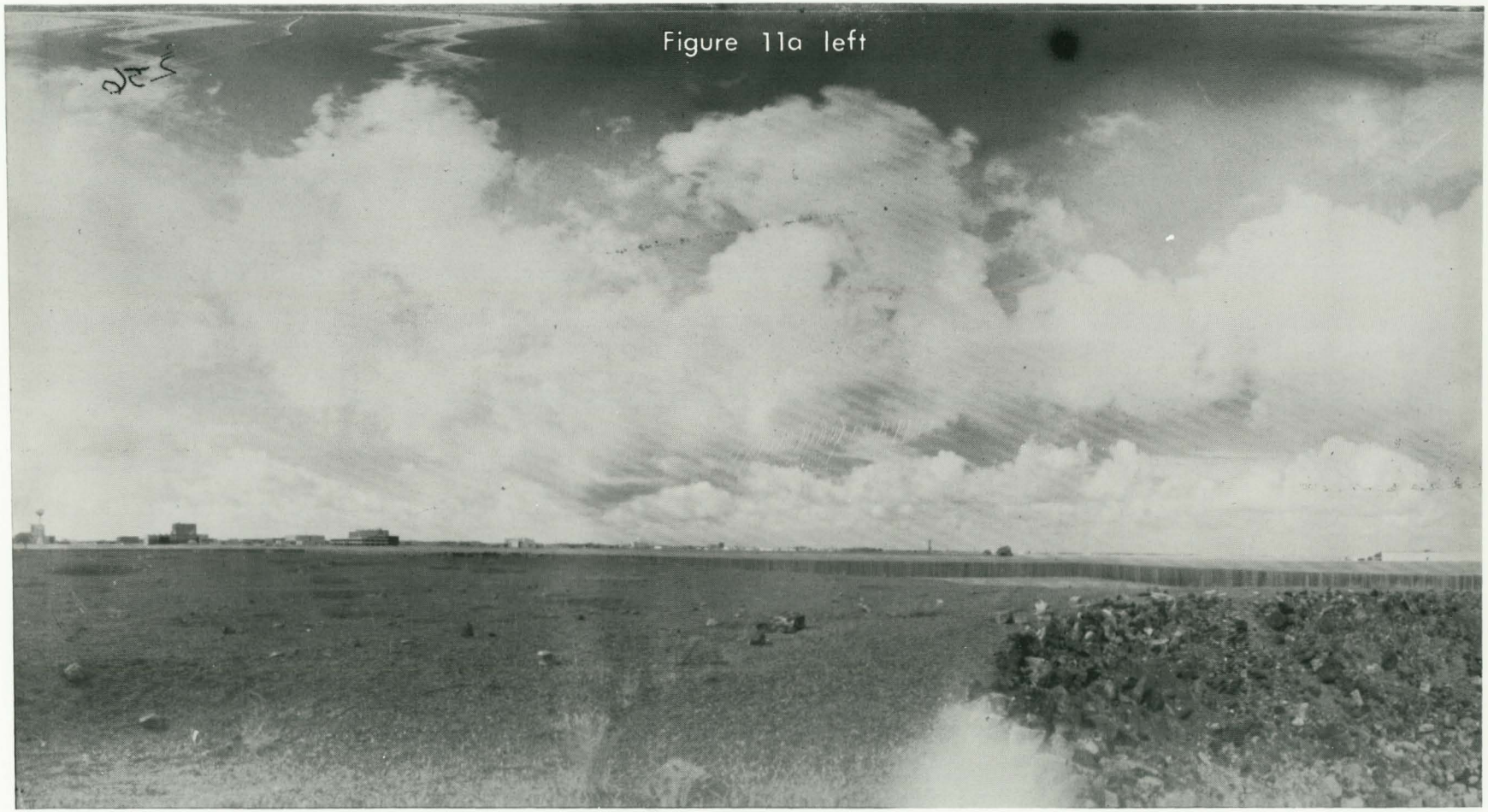
Figure 11a left

Figure 11a right

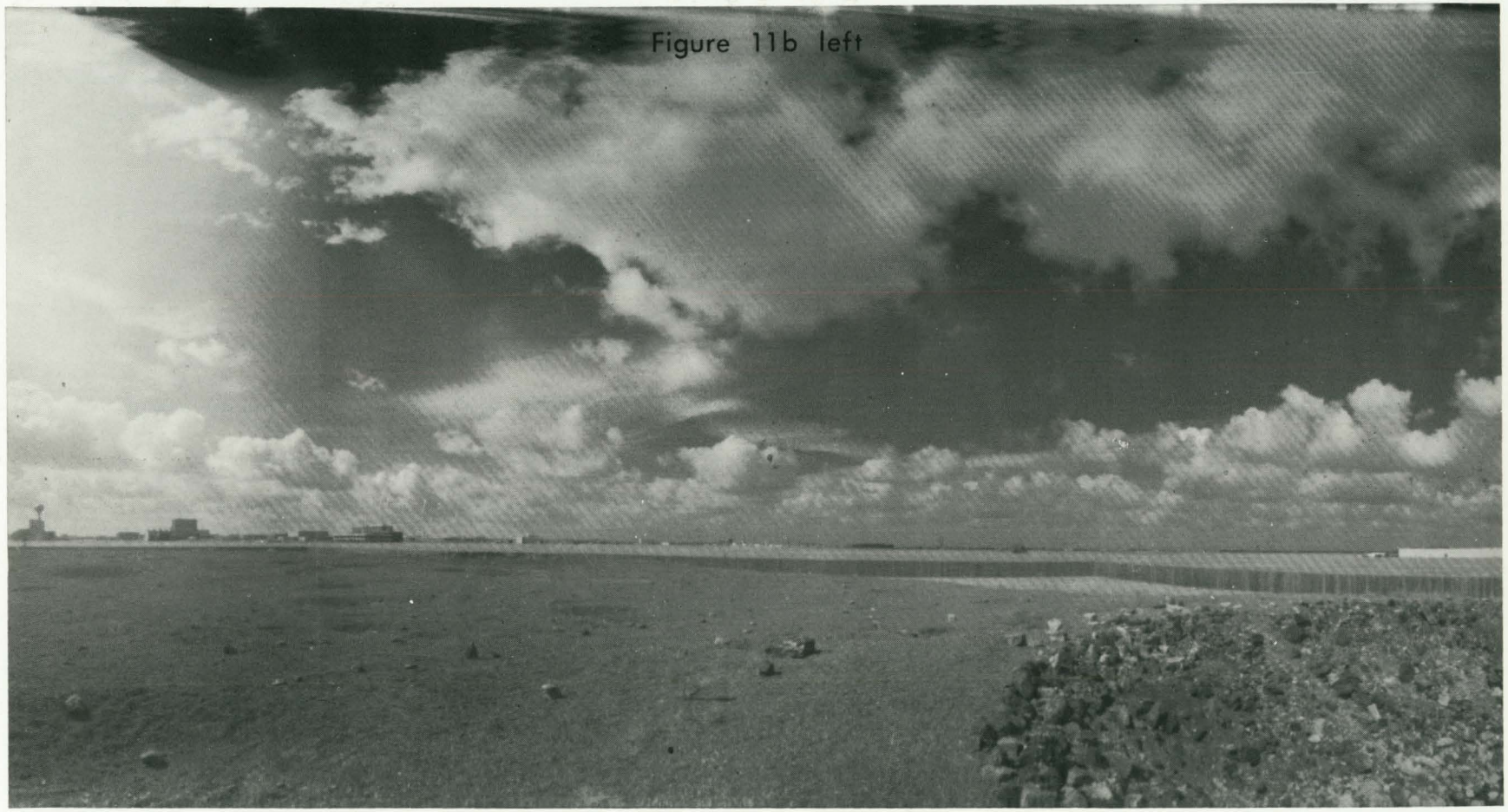
Figure 11b left

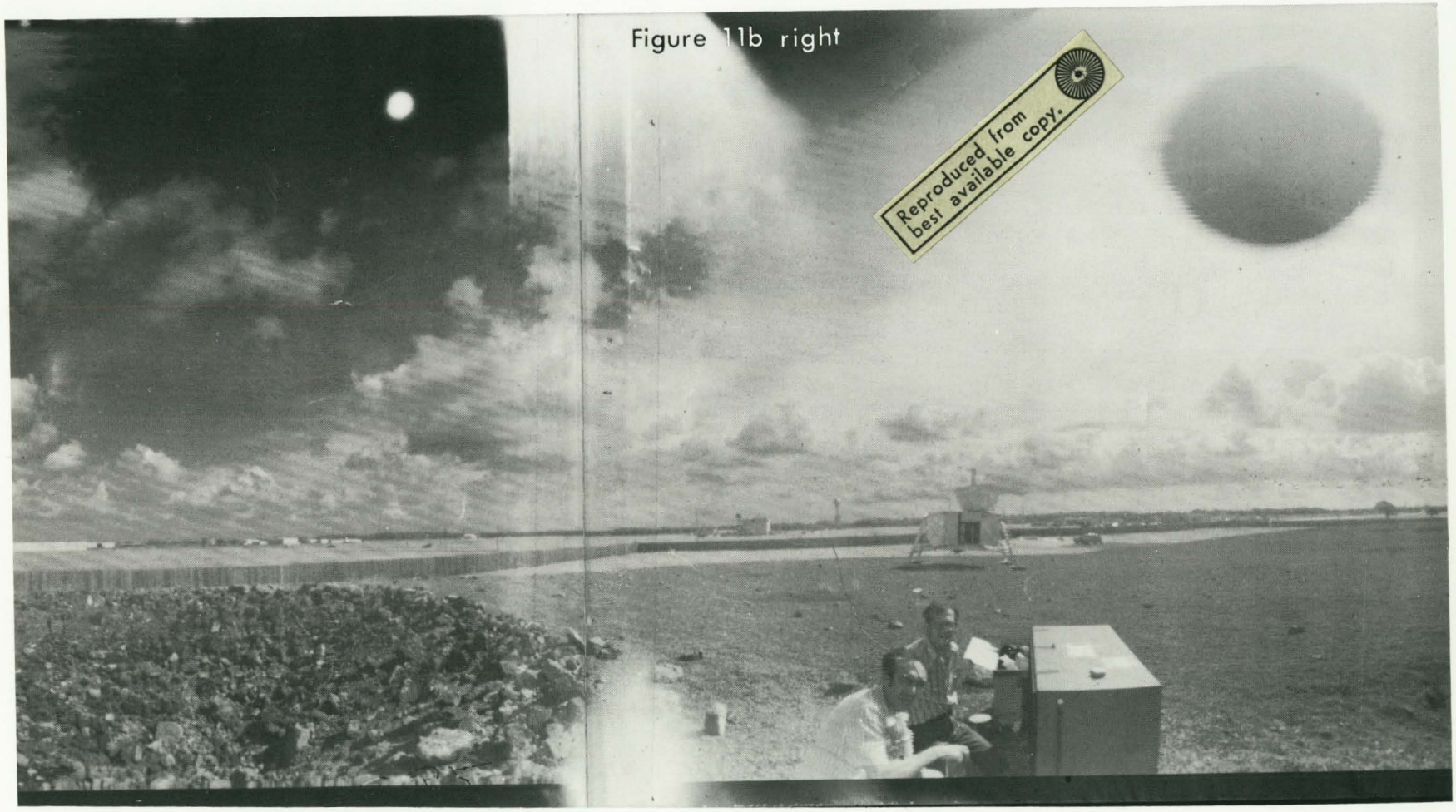
Figure 11b right
Reproduced from
best available copy.

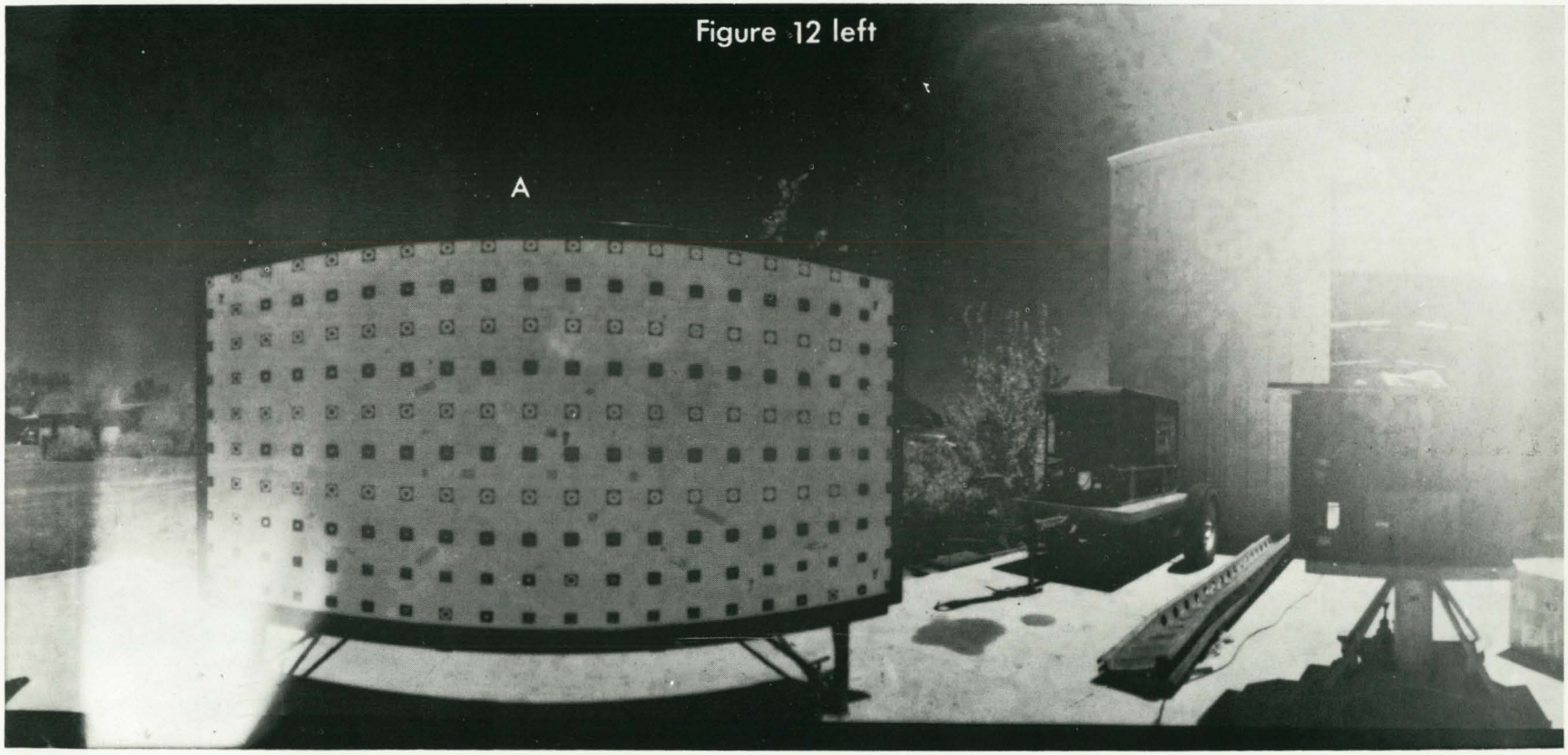
Figure 12 left
A

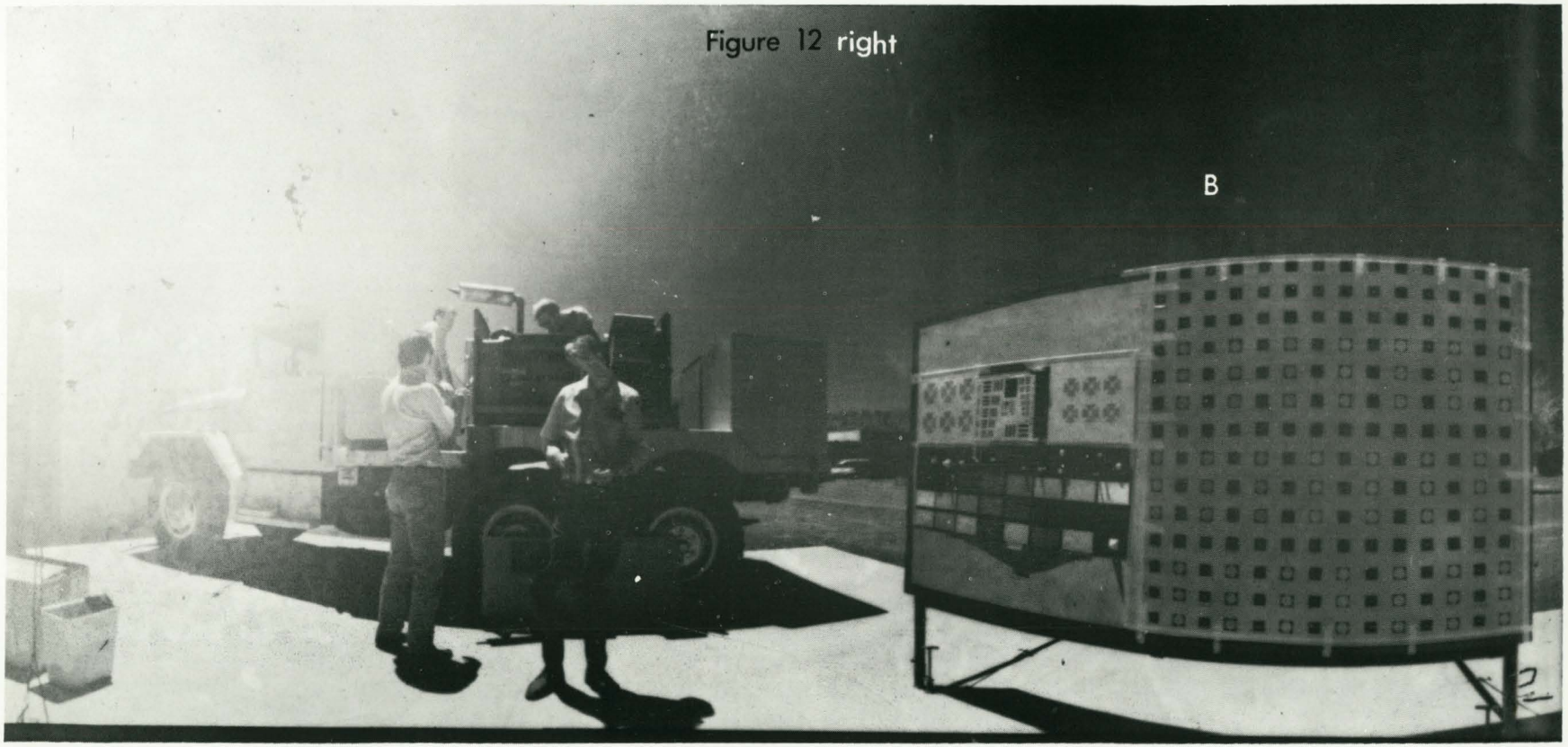
Figure 12 right
B

Figure 13